Science of the Total Environment 898 (2023) 165413

Contents lists available at ScienceDirect

Science of the Total Environment

journal homepage: www.elsevier.com/locate/scitotenv

Drivers of mangrove vulnerability and resilience to tropical cyclones in the North Atlantic Basin

Cibele Amaral [a,b,c,*], Benjamin Poulter [c], David Lagomasino [d], Temilola Fatoyinbo [c], Paul Taillie [e], Gil Lizcano [f], Steven Canty [g,h], Jorge Alfredo Herrera Silveira [i], Claudia Teutli-Hernández [j], Miguel Cifuentes-Jara [k,l], Sean Patrick Charles [d], Claudia Shantal Moreno [m], Juan David González-Trujillo [n,o], Rosa Maria Roman-Cuesta [p,q]

[a] Earth Lab, Cooperative Institute for Research in Environmental Sciences, University of Colorado Boulder, Boulder, CO 80303, United States
[b] Universidade Federal de Viçosa, Department of Forest Engineering, Viçosa, MG 36570-900, Brazil
[c] NASA Goddard Space Flight Center, Biospheric Sciences Laboratory, Greenbelt, MD 20771, United States
[d] East Carolina University, Department of Coastal Studies, Greenville, NC 27858-4353, United States
[e] University of Florida, Department of Wildlife Ecology and Conservation, Gainesville, FL 32611, United States
[f] Climate Scale, Parc Barcelona Activa, 08402 Barcelona, Spain
[g] Smithsonian Environmental Research Center, 647 Contees Wharf Road, Edgewater, MD 21037, United States
[h] Working Land and Seascapes, Smithsonian Institution, Washington, DC 20013, United States
[i] Centro de Investigación y de Estudios Avanzados, Departamento de Recursos del Mar, 97310 Mérida, Mexico
[j] Escuela Nacional de Estudios Superiores Unidad Mérida, 97357 Mérida, México
[k] Conservation International, Arlington, VA 22202, United States
[l] Centro Agronómico Tropical de Investigación y Enseñanza, 30501 Turrialba, Costa Rica
[m] Chair of Land Management, Technical University of Munich, Arcisstraße 21, D-80333 Munich, Germany
[n] Departamento de Biogeografía y Cambio Global, Museo Nacional de Ciencias Naturales, CSIC, JoseGutierrez Abascal, 2, 28006 Madrid, Spain
[o] Rui Nabeiro Biodiversity Chair, MED Institute, Universidade de Évora, Largo dos Colegiais, 7000 Évora, Portugal
[p] Wageningen University & Research, Laboratory of Geo-Information Science and Remote Sensing, 6708PB Wageningen, the Netherlands
[q] Technical University of Munich, School of Life Sciences, Institute of Forest Management, 85354 Fresing, Germany

ARTICLE INFO

Editor: Paulo Pereira

Keywords:
Remote sensing
Machine learning
Coastal ecosystem
Coastal development
Drought
Nature-based solutions

ABSTRACT

The North Atlantic Basin (NAB) has seen an increase in the frequency and intensity of tropical cyclones since the 1980s, with record-breaking seasons in 2017 and 2020. However, little is known about how coastal ecosystems, particularly mangroves in the Gulf of Mexico and the Caribbean, respond to these new "climate normals" at regional and subregional scales. Wind speed, rainfall, pre-cyclone forest height, and hydro-geomorphology are known to influence mangrove damage and recovery following cyclones in the NAB. However, previous studies have focused on local-scale responses and individual cyclonic events. Here, we analyze 25 years (1996–2020) of mangrove vulnerability (damage after a cyclone) and 24 years (1996–2019) of short-term resilience (recovery after damage) for the NAB and subregions, using multi-annual, remote sensing-derived databases. We used machine learning to characterize the influence of 22 potential variables on mangrove responses, including human development and long-term climate trends. Our results document variability in the rates and drivers of mangrove vulnerability and resilience, highlighting hotspots of cyclone impacts, mangrove damage, and loss of resilience. Cyclone characteristics mainly drove vulnerability at the regional level. In contrast, resilience was driven by site-specific conditions, including long-term climate trends, pre-cyclone forest structure, soil organic carbon stock, and coastal development (i.e., proximity to human infrastructure). Coastal development is associated with both vulnerability and resilience at the subregional level. Further, we highlight that loss of resilience occurs mostly in areas experiencing long-term drought across the NAB. The impacts of increasing cyclone activity on mangroves and their coastal protection service must be framed in the context of compound climate change effects and continued coastal development. Our work offers descriptive and spatial information to support the

* Corresponding author at: Earth Lab, Cooperative Institute for Research in Environmental Sciences, University of Colorado Boulder, Boulder, CO 80303, United States.
E-mail address: cibele.amaral@colorado.edu (C. Amaral).

https://doi.org/10.1016/j.scitotenv.2023.165413
Received 2 March 2023; Received in revised form 5 July 2023; Accepted 7 July 2023
Available online 8 July 2023

restoration and adaptive management of NAB mangroves, which need adequate health, structure, and density to protect coasts and serve as Nature-based Solutions against climate change and extreme weather events.

1. Introduction

Worldwide, mangrove forests buffer coastal areas and the human communities they support from wind, waves, and storm surges (Hochard et al., 2019; Menéndez et al., 2020; Zhu et al., 2020), while also storing carbon at some of the highest rates of any ecosystem (Donato et al., 2011; Richards et al., 2020). Globally, their coastal protection benefits are estimated to prevent US$ 60 billion in flood damages from tropical cyclones and shield 14 million people from their devastating impacts (Menéndez et al., 2020). Because of the high rate of storm occurrence and the vast extent of mangroves, flood mitigation benefits are particularly important to the countries of the North Atlantic Basin (NAB; Menéndez et al., 2020). Due to their structure and density, mangrove forests have the unique ability to slow down waves and wind, store water from surges, and reduce erosion by trapping sediments (Mazda et al., 1997; Thampanya et al., 2006; McIvor et al., 2012; Montgomery et al., 2019). This makes them one of the most effective Nature-based Solutions for coastal protection against climate change and extreme weather events, which include cyclone hazards (Earth Security, 2020; Van Hespen et al., 2023). However, their conservation remains a low priority in regional coastal planning policies and disaster risk reduction in the NAB. Simultaneously, the risk of tropical cyclones is predicted to increase in this region (Bacmeister et al., 2018; Emanuel, 2021; Knutson et al., 2021), where higher cyclone frequencies and intensities are already resulting in greater coastal damages (Wang and Toumi, 2021a, 2021b) affecting more exposed and increasingly more vulnerable communities (Hsiang and Jina, 2014; ECLA, 2018; Ötker and Srinivasan, 2018; Ramenzoni et al., 2020).

While mangroves are known to be resilient to the short-term impacts of tropical cyclones (Lugo, 1980; Jimenez et al., 1985; Roth, 1992; Krauss and Osland, 2020) and can even benefit from storm-induced nutrient loading (Castañeda-Moya et al., 2020), extensive and recurring mortality may suggest mangroves are less resilient to the long-term cyclone trends (Taillie et al., 2020; Lagomasino et al., 2021). For example, the 2017 Mega-Hurricane season resulted in 30 times more mangrove mortality than any year during 2009–2018 (Taillie et al., 2020). Some of this mortality may have resulted simply from storms happening to make landfall in areas of extensive mangroves. Still, other factors may have also played a role, including the preceding severe and long-lasting El Nino event in the region (2015–2016). This "drought-hurricane duo" may represent an interaction of multiple extreme events, which are particularly consequential in other tropical forests (Brando et al., 2014; Allen et al., 2021; Berenguer et al., 2021). Moreover, the nature of tropical cyclones in the NAB is thought to be changing in response to changes in climate, with more erratic and slow-moving storms bringing significantly higher amounts of rainfall (Hall and Kossin, 2019). The mangrove mortality resulting from this inundation is less well-understood than the more widely-documented impacts of wind damage (Roth, 1992; Imbert, 2018; Krauss and Osland, 2020; Lagomasino et al., 2021).

Because more recurrent damage to mangroves from tropical cyclones may compromise the buffering capacity of mangroves to future cyclonic events (Danielson et al., 2017), it is imperative to identify regional hotspots of cyclone-driven mangrove vulnerability (i.e., propensity to damage) and loss of resilience (i.e., loss of capacity to recover after damage). Additionally, there is a need to identify the drivers of widespread mangrove damage and loss of resilience after tropical cyclones to define the best management for each case while enhancing mangrove functionality and persistence (Gijsman et al., 2021).

In this context, "damage" refers to a decrease in mangroves' greenness signal (Normalized Difference Vegetation Index (NDVI)) following a cyclone impact that falls below a certain threshold compared to their baselines. The damage indicates how vulnerable the mangroves are to a cyclone's impact. "Loss of resilience" describes a situation in which mangroves lose their capacity to recover from the damage (Ingrisch and Bahn, 2018), resulting in a null or negative trend in their greenness signal after the damage. The NDVI is a useful ecosystem resilience proxy since it highly correlates with leaf area index, species richness, and aboveground net primary productivity (Yengoh et al., 2015; Almeida et al., 2021). It has been used to characterize mangrove damage and recovery from extreme weather events worldwide (e.g., Goldberg et al., 2020; Taillie et al., 2020; Adame et al., 2021; Lagomasino et al., 2021).

Previous research has shown that mangroves in the NAB are more vulnerable to cyclone impact if 1) they are structurally taller than surrounding trees, 2) wind speeds are $\geq$100 km h^{-1}, 3) storms cause widespread flooding, 4) cyclone recurrence is relatively low (only affected by a few cyclones before), and 5) the species composition is dominated by red mangrove (*Rhizophora mangle* L.) (Smith et al., 2009; Imbert, 2018; Sippo et al., 2018; Rivera-Monroy et al., 2020; Taillie et al., 2020; Lagomasino et al., 2021; Peereman et al., 2022). On the other hand, mangroves exhibit loss of resilience after being damaged if they are 1) located in poorly drained basins that are prone to impounding of high salinity storm surge, 2) in areas with lower fertility, or 3) where species composition is dominated by black or white mangrove (*Avicennia germinans* (L.) L., *Laguncularia racemosa* (L.) C.F. Gaertn.) (Smith et al., 2009; Harris et al., 2010; Vogt et al., 2012; Imbert, 2018; Rivera-Monroy et al., 2020; Lagomasino et al., 2021). However, cyclones and site properties may have different impacts on NAB mangrove species in other conditions. These three main species vary in ecological and biomechanical properties. *R. mangle*, commonly situated on the lower to mid-intertidal zone along shoreline edges, possesses prop roots that offer stability and oxygen supply to the root zone. *A. germinans*, on the other hand, is typically located at slightly higher elevations in the upper intertidal zone and may experience flooding conditions. This species features horizontal cable roots that protrude pneumatophores, or stick-like aerial roots, up to 30 cm above the soil surface to provide oxygen to the root zone. It also has a salt excretion mechanism that helps the tree to tolerate the high salinity. *L. racemosa*, which is typically situated at higher elevations than the other two species and is rarely flooded, may not have visible roots but can produce prop roots if flooded for prolonged periods or subjected to anaerobic soil conditions (Tomlinson, 2016; Tomiczek et al., 2021). *R. mangle* presents thinner stems with higher mechanical resistance when compared with *A. germinans*, a tree species with wide girth and flare at the base (Méndez-Alonzo et al., 2015), while L. *racemosa* possesses a flexible and adaptive biomechanical structure that enables it to withstand strong winds (Spatz et al., 1987).

While the previous studies help to understand broader patterns in mangrove vulnerability and resilience to tropical cyclones in the NAB, they are also limited in that they 1) have only captured the responses on specific sites and/or one-year post-disturbance responses and 2) have mainly included environmental variables and short-term climate responses without assessing long-term climate trends and human drivers such as the influence of urbanization, croplands, and road networks, which are also known to act as drivers of mangrove degradation and loss (Feller et al., 2015; Hayashi et al., 2019; Branoff, 2020; Goldberg et al., 2020; Villate Daza et al., 2020).

Building on these important findings from previous work, we aimed to leverage the growing library of freely-available spatial data to investigate broader, more generalizable patterns in mangrove vulnerability and resilience. Specifically, we pose four major questions: 1) What is the extent of tropical cyclone (i.e., tropical storms and hurricanes)

impact on mangroves in the North Atlantic Basin between 1996 and 2020? 2) Where are cyclone impacts, mangrove damage, and post-disturbance loss most pronounced? 3) What are the drivers and thresholds of mangrove vulnerability? And 4) What are the drivers and thresholds of mangrove post-disturbance resilience? Answers to these questions at the regional and subregional levels are critical to risk assessments, adaptation policies, and ecosystem restoration and conservation across the NAB.

2. Material and methods

2.1. Study site

Our study focused on mangrove forests of the Caribbean and the Gulf of Mexico regions. These regions cover an area of 7,741,775.5 km^2 from South to North America (i.e., 7–30°N and 60–98°W), host 35 countries, and can be subdivided into nine coastal ecoregions, according to Spalding et al. (2007) (Table A.1). This bioregionalization was created to support national and international conservation policy agendas and are based on global biogeographic patterns (Spalding et al., 2007). In 1996, the first year of our study, the NAB was estimated to include 2,025,295 ha of mangroves (Bunting et al., 2018). Of the coastal subregions, the Southern Gulf of Mexico and the Greater Antilles supported the largest extents of mangroves, while the Northern Gulf of Mexico supported the least mangroves (Table A.1).

In addition to varying in mangrove extent, the coastal ecoregions varied in several relevant climate and human infrastructure variables (Table A.1). The Bahamian, Floridian, and Northern Gulf of Mexico were notable for the highest cumulative wind speeds, while the Southwestern and Western Caribbean subregions were notable for the highest cumulative rainfall from hurricane seasons in the last 40 years (Hersbach et al., 2023). The region as a whole had a mean annual maximum temperature of 29.5 °C and a mean annual rainfall of 126.7 mm (CRU et al., 2017), and both temperature and rainfall patterns followed a decreasing latitudinal gradient. The region as a whole experienced a period of significant drying (Neelin et al., 2006), with the Bahamian, Greater Antilles, and Western Caribbean subregions experiencing the highest drought tendencies (Table A.1). The region hosted a total of 1293 human settlements (CIESIN et al., 2011) with 41,801 km of roads within 5 km of the coastline (CIESIN and ITOS, 2013). While the Northern Gulf of Mexico supported the largest number of coastal settlements, the Greater Antilles had more roads in the coastal zone (Table A.1).

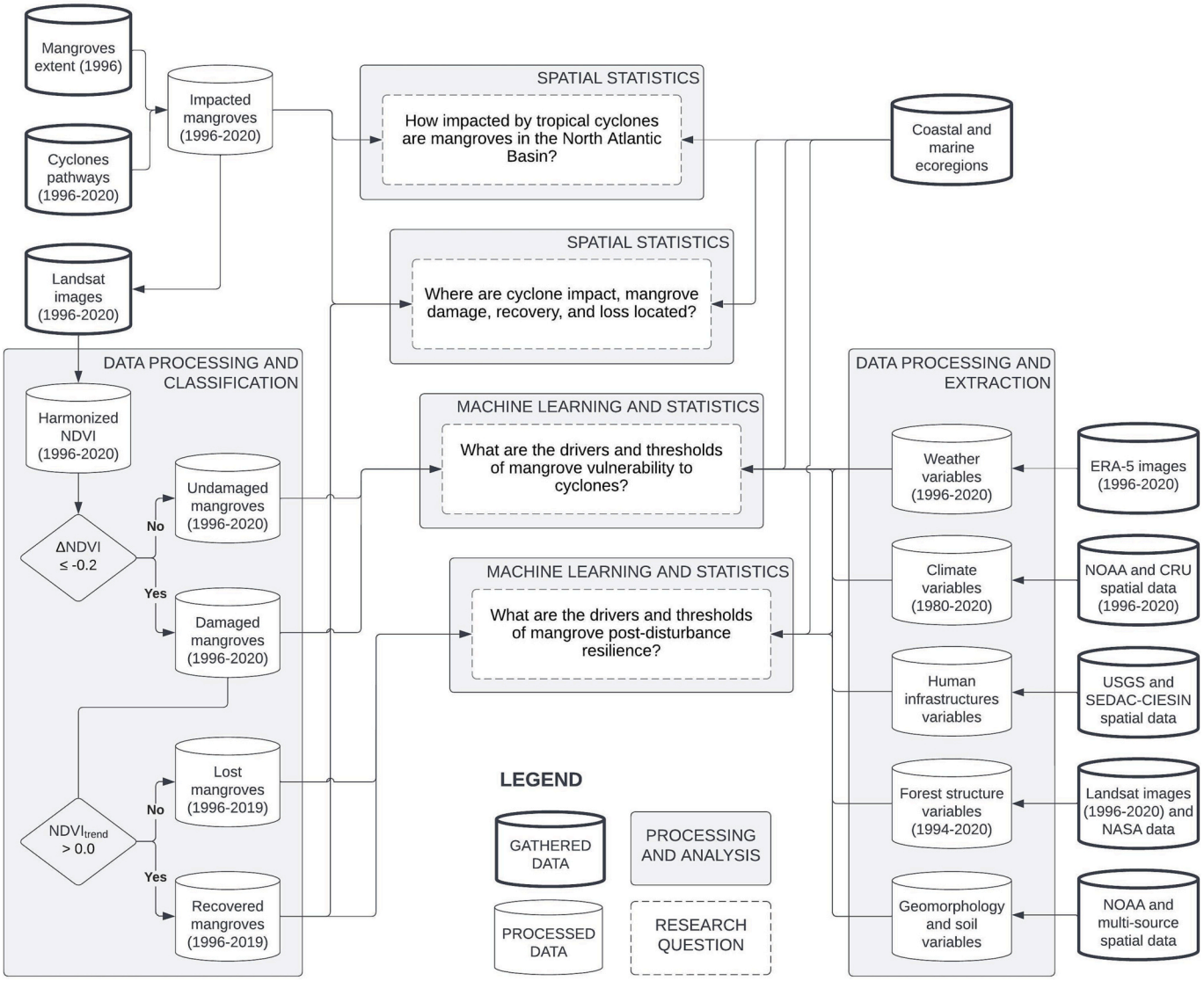

Fig. 1. Workflow diagram. Detailed information on the data used in this study is presented in Table A.2.

2.2. Methods

To identify the hotspots of cyclone impact, mangrove damage, and mangrove loss, as well as the environmental drivers of these ecosystem responses, we analyzed remote sensing and spatial data collected over 25 years. We used spatial statistics, descriptive statistics, and machine learning to quantify patterns across the entire NAB and its subregions (Fig. 1).

2.2.1. Mangrove vulnerability and short-term resilience classification

We calculated changes in forest greenness through the Normalized Difference Vegetation Index (NDVI) obtained from 30-m resolution, harmonized Landsat-5, −7, and −8 images to identify damage in impacted mangrove areas, which have been proven reliable to monitor mangrove damage and recovery (e.g., Taillie et al., 2020; Lagomasino et al., 2021). Based on ground-validated responses (Lagomasino et al., 2021), mangrove damage (vulnerability, i.e., the potential of damage when exposed to a tropical cyclone) followed a threshold change response of −0.2 NDVI (a drop-response of 0.2) between the *ex-ante* NDVI mean value (two years before the disturbance, July 1 to July 1, i.e., the baseline) and the *ex-post* NDVI mean value (from August 31 to December 31, i.e., the hurricane season). This 0.2 decline in NDVI following the cyclone has been reported to show a significant change in canopy cover fraction and canopy height loss (Taillie et al., 2020; Lagomasino et al., 2021) (see example in Fig. A.1) and has been used as a mangrove loss threshold in different mangrove degradation assessments (e.g., Lagomasino et al., 2019; Goldberg et al., 2020; Taillie et al., 2020; Adame et al., 2021; Lagomasino et al., 2021). To measure recovery (short-term resilience, i.e., the capacity to recover from the disturbance), we focused on the *ex-post* NDVI slope trend for eight months after the damage (from January 1 to August 31). A negative NDVI trend (or null trend) was classified as loss (i.e., persistent damage with no recovery signal), and a positive trend as recovery (i.e., damaged with signals of recovery) (Taillie et al., 2020). While our short-term losses do not necessarily lead to long-term mangrove mortality, experience in the region showed that eight months following the end of the hurricane season was a reasonable time to expect recovery responses (Lagomasino et al., 2021). Damage and recovery were produced annually at 30-m spatial resolutions for the periods 1996–2020 and 1996–2019, respectively, for the entire NAB region.

We used Global Mangrove Watch (GMW) data (Bunting et al., 2018) for our mangrove baseline (the year 1996). Tropical cyclones were collected from NOAA's-IBTrACS (Knapp et al., 2010) and include both tropical storms (wind speed 63–117 km.hr^{-1}) and hurricanes (wind speeds $\geq$ 119 km.h^{-1}), following the Saffir-Simpson scale. Because no information is available on the historical tracks' wind radii pre-2008, a set 160 km buffer (80 km on either side of the storm track) was used to estimate the potential area of influence around the storm, i.e., the area of cyclone impact. The median size of Atlantic cyclones based on the outermost isobar is 278 km for tropical storms and 370 for category 1 and 2 storms (Landsea et al., n.d.). The buffer used here is closer to the average 34-knot wind speed radii for the top 73 most costly Atlantic cyclones before the 2017 season, of 216 km (Zhai and Jiang, 2014). The extreme variability in storm size makes it difficult to quantify a particular storm's exact area of influence, but using the standard buffer size of 160 km allows for a systematic comparison across individual years. Class point data (i.e., pixel centroids) were randomly extracted from the aggregated layers (1996–2020) to assess the drivers of vulnerability and loss of resilience for the NAB region and subregions (Spalding et al., 2007) in a space-by-time approach. The analysis of the subregions was considered highly relevant due to the large differences in environmental settings (e.g., soil type, mean elevation, geomorphology), frequency of cyclones, socio-economic frameworks, and governance settings among them.

2.2.2. Spatial statistics

Several spatial statistics were used to assess the history of cyclone impact, mangrove damage, and post-disturbance recovery and loss across the NAB and its subregions. We calculated the accumulated area impacted by tropical cyclones per subregion by summing the annual impacted mangrove area layers from 1996 to 2020. We mapped the hotspots of cyclone impact, mangrove damage, and loss using the related annual layers from 1996 to 2019. They were created from the union of the 24 annual layers. Thus, the annual occurrences of damage, recovery, and loss were registered in the 1996–2019 layers and the sum of the years of occurrence. We created a 0.5-degree grid and calculated the times (recurrence) of tropical cyclone impact per cell, the ratio (percentage) of mangrove damage/cyclone impact per cell, and the ratio of mangrove loss/damage per cell. To allow the comparison between maps, we did not map the impacts and damages of the 2020 season (please, see Section 2.2.1 for detailed information on short-term loss layer calculation).

2.2.3. Drivers of mangrove vulnerability and short-term resilience

2.2.3.1. Weather variables – the year of the cyclone's impact. Weather variables during the year of a given cyclone were extracted from the Copernicus Climate Change Service (C3S) Climate Data Store (CDS) ERA5 reanalysis with 0.25° of spatial resolution and hourly temporal resolution (Hersbach et al., 2018). We produced annual maximum sustained wind speed images from 1996 to 2020 from ERA5's hourly wind data, which summarizes the maximum 3-s wind at 10-m height (Hereafter referred to as 'wind speed'). We developed two cumulative rainfall products per year, one from May to November (referred to as the 'hurricane season') and one for December to April ('dry season'). For mangroves with repeated cyclone impacts, we estimated mean wind speed and cumulative rainfall values for each pixel. For the 'undamaged' class, we took mean values from the 25-year period of analysis.

2.2.3.2. Climate variables – Long-term means and trends. We calculated the number of times each pixel intercepted a 80-km-wide buffer along the pathway lines of the cyclones to estimate the recurrence of tropical cyclones over the 25 years. Five other variables were calculated to capture long-term climate variability in the region: 1) mean annual maximum temperature (°C), 2) the trend of the annual maximum temperature (°C.yr^{-1}), 3) mean annual cumulative rainfall (mm), 4) the trend of the annual cumulative precipitation (mm.yr^{-1}), and 5) the trend of the annual mean Self-calibrating Palmer Drought Severity Index (scPDSI) (unitless, but a negative trend indicating drought) from 1980 to 2016. We used monthly data from the Climatic Research Unit (CRU et al., 2017) database at 0.5° spatial resolution.

2.2.3.3. Human infrastructure variables. To determine the impact of coastal development on mangroves during tropical cyclones, we created layers of distance from human infrastructures. Our analysis involved calculating Euclidean distance from croplands, roads, and settlements at a spatial resolution of 100 m. The original cropland mask came from the global croplands project, version 1, at 30 m spatial resolution from 2010 (North America; Massey et al., 2017) and 2015 (South America; Zhong et al., 2017). Croplands with an area lower than one hectare were excluded to reduce feature complexity and allow the generation of a single-distance raster for the entire region. Road polyline data were taken from the 'Global Roads Open Access' dataset, version 1, with accuracies ranging from 530 m to 1265 m (CIESIN, 2013). We used settlement point data from the Global Rural-Urban Mapping Project version (CIESIN, 2011).

2.2.3.4. Forest structure variables. We included four pre-cyclone forest structure variables: one for canopy height and three for canopy cover (i.e., the fractional cover of green vegetation, soil, and water). We used

data on mangrove canopy height from NASA's ORNL DAAC (Simard et al., 2019a, 2019b), derived from the Shuttle Radar Topography Mission (SRTM) and the RH100 product from the Geoscience Laser Altimeter System (GLAS) instrument aboard ICESat-1. This data is from 2000 at a 30-m resolution. We utilized Spectral Mixture Analysis (SMA) (Adams et al., 1986) to generate sub-pixel fractional covers of green vegetation, soil, and water classes. This helped us determine the pre-cyclone canopy cover. We used two sets of 100 candidate spectra collected across the region and years/seasons to do this. We applied each dataset to Landsat-5 collection 1, tier 1 (from 1994 to 2011) and Landsat-8 collection 1, tier 1 (from 2013 to 2020). We ran the images unmixing using Google Earth Engine 'unmix' function (Gorelick et al., 2017; Bullock et al., 2020). To identify a representative endmember for each class, we utilized the Endmember Average RMSE (EAR) method (Dennison and Roberts, 2003). This involved calculating the EAR for each endmember by taking an average of the RMSE from models that utilized that particular endmember to unmix spectra belonging to the same class. The EAR for Landsat-5 endmembers ranges from 0.011 to 0.020, while for Landsat-8, it varies from 0.011 to 0.063. When dealing with mangrove samples that have experienced multiple damage, short-term loss, or recovery over time, we assigned the pre-cyclone fractional cover to the first cyclone impact since 1996.

2.2.3.5. Geomorphology and soil variables. We selected four geomorphological typologies: Delta, Estuary, Lagoon, and Open Coast, obtained from Worthington et al. (2020). These data were produced using high-resolution coastline layers to map and classify coastal embayment polygons through machine learning. We also generated a 100-m spatial resolution layer of Euclidean distance to the shoreline using the Prototype Global Shoreline Data (https://shoreline.noaa.gov/data/datasheets/pgs.html). It is based on orthorectified, 2000-era, Landsat imagery and has an accuracy of ca. 50 m.

We include data on soil organic carbon stocks at 1-m depth from the global mangrove forest soil carbon map at 30 m spatial resolution (Sanderman et al., 2018). This database was produced by the 250-m SoilGrid data modeling from various finer resolution explanatory variables such as a digital elevation model, geomorphology map, and vegetation characteristics. The data presents a soil organic density root mean squared error (RMSE) of 10.9 kg/m^3.

2.2.3.6. Correlation matrices. We applied nonparametric Spearman and Kendall Rank Correlation tests to exclude highly correlated possible variables, ending with a final pruned set of 22 possible drivers (see a summary of the variables' characteristics and sources in Table A.2 and correlation matrices in Figs. A.2 and A.3). The set of variables used here represents a large number of possible direct and indirect drivers of mangrove health conditions in the region – which could influence the ecosystem vulnerability and resilience to tropical cyclones impact – while fitting to the spatial and temporal scales of the research.

2.2.4. Machine learning and statistical analyses

We used the machine learning algorithm Random Forest (RF) to relate variables to mangrove damage and loss (Breiman, 2001; Kuhn et al., 2020) and then calculated descriptive statistics (i.e., median and

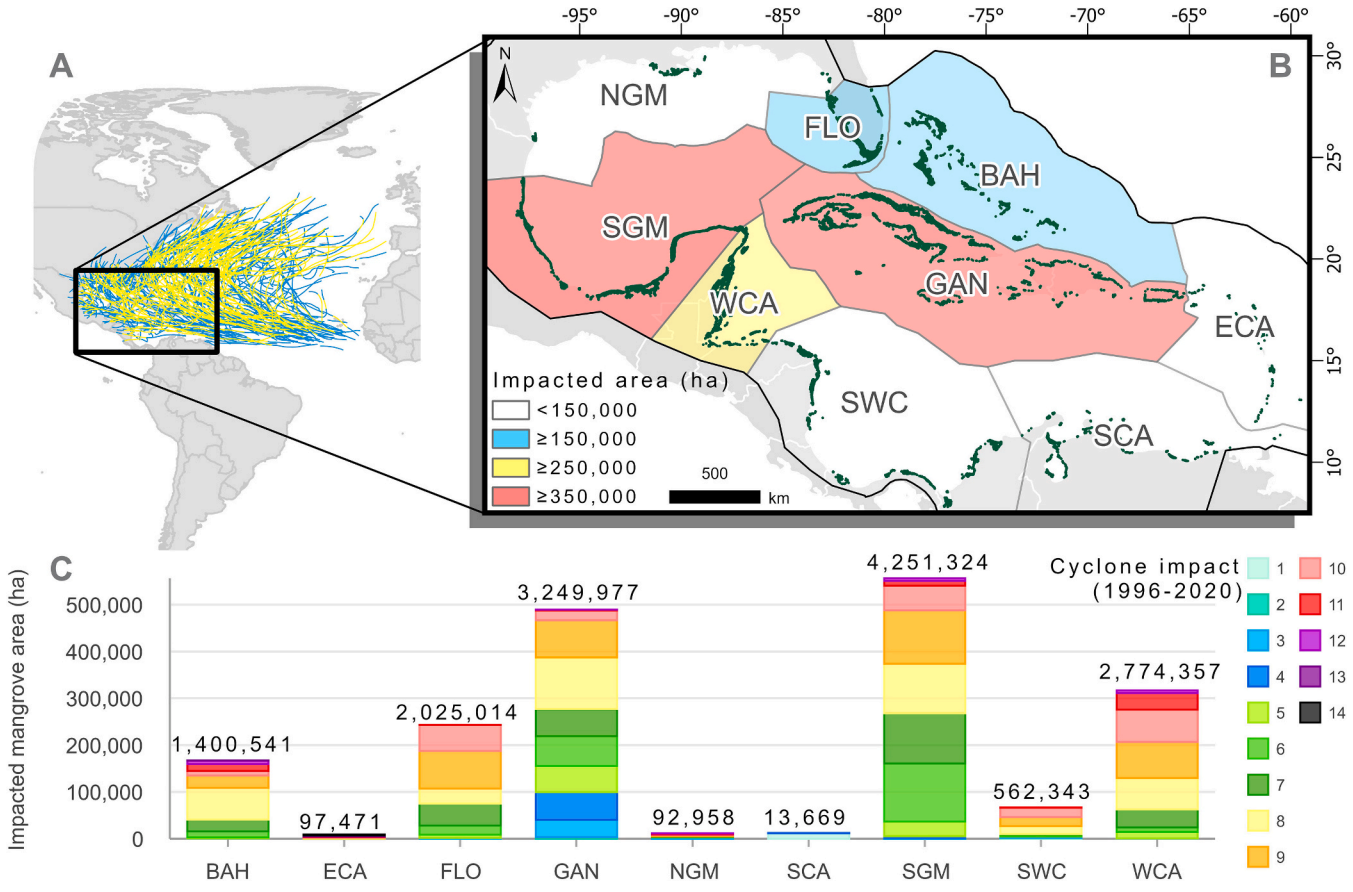

Fig. 2. Study site and impact of tropical cyclones on NAB mangroves: A) Atlantic named cyclones' pathways (from storms – in blue to hurricanes – in yellow) from 1996 to 2020, and study site location (black box). B) Zoom-in of the study site showing the distribution of mangroves (in dark green, from Bunting et al. (2018)) and its nine subregions colored according to ranges (from <150,000 to ≥350,000 ha) of mangrove area impacted over the last 25 years. C) Cumulative mangrove area impacted by tropical cyclones per subregion (label) with stacked color bars indicating how many hectares have been impacted by cyclones successively (from one to fourteen times) in the last 25 years. Subregion full names are listed in Table 1.

quartiles per class of vulnerability and recovery), non-parametric statistic tests (Kruskal-Wallis for numerical, and Chi-squared for categorical variables) to characterize and select the most influential drivers of vulnerability and resilience for the NAB region and the subregions. Not all nine subregions hosted enough mangrove data to run RF that required balanced control vs. treatment subsamples. Five subregions, comprising 94 % of the total mangrove area in the region, were used for running subregional models: the Bahamian, Floridian, Greater Antilles, Southern Gulf of Mexico, and the Western Caribbean (Fig. 2). Thus, twelve models were run: one regional and five subregional models for vulnerability ("damaged vs. undamaged mangroves") and for post-disturbance resilience ("recovered vs. lost mangroves") (Table A.3).

We set 700 trees per model and left the number of predictors at each split to be selected based on the highest overall accuracy. We used 10-fold cross-validation (10 % of data hold-out for validation) to assess the accuracy of the models. The relative importance of different drivers relied on the difference between two prediction accuracies on the out-of-bag portion of the data for each tree when permuting each predictor variable (Kuhn, 2012). All data analyses were performed using R 4.0.0 (R Core Team, 2020).

3. Results

3.1. Impact of tropical cyclones on NAB mangroves

From 1996 to 2020, the NAB region experienced 368 named tropical cyclones (87 are category ≥3, i.e., wind speed ≥178 km.h^{-1}) (Fig. 2A and B). Of the 2 million hectares of mangroves in the NAB originally (Bunting et al., 2018), almost all (93 %) were impacted by at least one cyclone landfall. Half of that area (55 %) was impacted by eight or more landfalls in the 25-year study period (Fig. 2C and Table 1). Geographically, the Eastern Caribbean subregion experienced the highest number of landfalls: 14 in 25 years (Figs. 2C and 3A). These results illustrate the important role of cyclone return intervals in mangrove dynamics. The highest absolute areas of impacted mangroves correspond to subregions with larger mangrove extents: the Southern Gulf of Mexico and the Greater Antilles, with ca. 500,000 ha of impacted mangroves each. (Fig. 2C and Table 1).

3.2. Hotspots of cyclone impact, mangrove damage, recovery, and loss located

While cyclone landings affected almost all mangroves in the NAB region (Fig. 3A), the vulnerability was low, illustrating that mangroves are well-adapted to the impact of cyclones. Hence, damage represented a small percent of the total area of impacted mangroves, with 14.9 % (279,914 ha) of mangroves damaged at least once during our 25-year analysis period. The central-eastern side of the NAB (Eastern Caribbean, Bahamian, Greater Antilles) concentrated the highest ratios of mangrove damage (damage/impact) with values above 20 % (Table 1 and Fig. 3B). The Southern Caribbean subregion received little to no impact as this region is located outside the path of the most frequent cyclone occurrence. The Eastern side of the Caribbean, mainly, and the Western Caribbean act as preferential pathways for cyclones.

Regional mangrove resilience was, however, rather low, with rates of post-disturbance loss (loss/damage) being ca. 48 % (Table 1). A total of 123,885 ha of mangroves showed no recovery trends in the following eight months after the disturbance. Maximum resilience was observed in the Floridian subregion, with 78.4 % of the recovery, while the lowest values were within the Bahamian (32.4 %) and Eastern Caribbean (45.6 %) subregions (Table 1). In absolute numbers, mangrove-rich central-western subregions (i.e., the Greater Antilles, the Western Caribbean, and the Southern Gulf of Mexico) contributed the most to mangrove losses (Table 1 and Fig. 3C). The central-eastern region is notable for its high loss of resilience after damage, especially in the Bahamian (BAH) subregion (Fig. 3C).

3.3. Drivers and thresholds of mangrove vulnerability to cyclones

Mangrove vulnerability to tropical cyclones for the period 1996–2020 was mostly influenced by weather properties linked to the cyclonic events: wind speeds and high rainfall, which often causes flooding (detailed information on each vulnerability model, accuracies, and descriptive statistics are presented in Tables A.4 to A.10). These were common drivers for the NAB region (Fig. 4A) and all the subregions (Fig. 4B to F). The importance of wind speed and rainfall was greatest in the subregions located on the preferential pathway of cyclones in the NAB region (eastern side of the Caribbean), the Bahamian, Eastern Caribbean, Greater Antilles, and Floridian subregions (Fig. 4B to D). Many of these subregions comprise islands and peninsulas, allowing cyclones to pass over them without losing much intensity. More continental subregions, such as the Southern Gulf of Mexico or the Western Caribbean, saw wind speed and high rainfall as leading drivers of vulnerability. Still, long-term climate trends, human infrastructure, geomorphology, and pre-cyclone forest (height and canopy openness), were the most important drivers of mangrove vulnerability to tropical cyclones (Fig. 4E and F).

3.3.1. Thresholds of vulnerability at the regional level

Translated into thresholds for the NAB region, we found that mangrove vulnerability to tropical cyclones was enhanced by insularity with wind speeds ≥107 km.hr^{-1}, and high levels of associated cyclonic rainfall (~1050 mm) strongly driving mangrove damage (Fig. 5A and B). Taller mangroves (~10 m) were more vulnerable than shorter mangroves (Fig. 5C), and lagoonal mangroves were more damaged than open coast, estuaries, and delta mangroves (Fig. 5D).

3.3.2. Thresholds of vulnerability at the subregional level

On a subregional level, the results of our models showed that wind speed and rainfall interact at multiple timescales to influence mangrove vulnerability (e.g., rainfall during the hurricane season, rainfall preceding the hurricane season, and long-term rainfall trends). The Bahamian subregion was the most vulnerable. There, rainfall was as important as wind speed in driving mangrove damage, which was a unique subregional response (Fig. 4B). Thus, mangroves in the Bahamian subregion were highly responsive to cumulative rainfall during the hurricane season: 1218 mm vs. 763 mm in damaged and undamaged areas, respectively. Shorter mangroves (~1.7 m tall) were more vulnerable than taller mangroves (~6.8 m), an exception to the general rule within the NAB. Long-term drought also conditioned the vulnerability of Bahamian mangroves, where damage was more frequent in areas undergoing decreasing rainfall since the '80s: median of −0.05 mm.yr^{-1} vs. 0.04 mm.yr^{-1} in damaged vs. undamaged mangroves (Table A.6). Rainfall also conditioned vulnerability in other subregions, such as the Southern Gulf of Mexico, where aridity played a role. Thus, mangroves experienced more damage in areas with lower median annual rainfall (ca. 77 mm) than higher annual means (118 mm) (Table A.9).

Human drivers also influenced the vulnerability of mangroves in less insular subregions such as the Southern Gulf of Mexico and the Western Caribbean subregions, where damage was more likely in mangroves closer to settlements (16 vs. 31 km, damage vs. undamaged, respectively) (Fig. 4F and Table A.10). Human variables were also key in the Bahamian subregion, where damaged mangroves were up to four-times closer to human infrastructure and to crops than undamaged mangroves in the Bahamian region (Fig. 4B and Table A.6).

Geomorphology was very influential in the Greater Antilles subregion, where 71 % of the damaged mangroves were in lagoonal settings, while 60 % of the undamaged mangroves were on the open coast. Regarding the Western Caribbean, the proximity of mangroves to the shoreline plays a significant role in their susceptibility to damage. Those situated closer to the sea (around 440 m nearer) are at a higher risk of being damaged than those located farther away. (Fig. 4F).

3.4. Drivers and thresholds of mangrove post-disturbance resilience

Short-term mangrove resilience for the period 1996–2019 showed a far greater diversity of influences at regional and subregional scales (Fig. 6A vs. Fig. 4A), highlighting the importance of local conditions in driving short-term resilience, in contrast to the more uninformed role of weather-related cyclonic properties for vulnerability (detailed information on each recovery model, accuracies, and descriptive statistics are presented in Tables A.11 to A.17). Human drivers, pre-cyclone forest structure and geomorphology all played influential roles in the NAB and subregional resilience. Regionally, the most remarkable novel influence on mangrove recovery was the understudied role of long-term climate trends (e.g., annual cumulative rainfall, Self-Calibrated Palmer Drought Severity Index (scPDSI), and annual maximum temperature). These three variables suggested that mangroves were less resilient to tropical cyclones in sites with drought and heat trends (Fig. 7A and B). For example, positive trends in scPDSI (0.03 ΔscPDSI.yr^{-1}) were associated with resilience, while areas suffering from drying trends (−0.02 ΔscPDSI. yr^{-1}) saw no recovery eight months after the disturbance. Other drivers of regional resilience also included wind speed, with stronger cyclones (hurricanes cat ≥3, wind ≥178 km.hr-^{1}) leading to higher mangrove recovery. Geomorphology was as important for recovery as vulnerability, with basin mangroves farther from the coast, such as lagoonal mangroves being less resilient (Table A.12).

3.4.1. Thresholds of resilience at the regional level

Site conditions played major roles in defining resilience. Mangrove stands with taller trees (13.6 m for recovered mangroves vs. 8.5 m for non-recovered), denser canopies (75 % of the recovered mangroves had pre-cyclone green vegetation fractions above 80 %), and higher soil organic carbon stocks (522 vs. 509 Mg C. ha-1 for recovered vs. non-recovered, respectively) recovered better after disturbance (Fig. 7C to F). Distance to the coastline was an important regional variable influencing mangrove resilience, with mangroves closer to shore recovering more quickly after cyclones (Table A.12).

3.4.2. Thresholds of resilience at the subregional level

Human infrastructure was a key predictor of mangrove resilience across all subregions (Fig. 6). As was observed for vulnerability, the Bahamian subregion showed clear responses to infrastructure. This was also the case for the Southern Gulf of Mexico and Western Caribbean subregions, where human variables displayed >80 % of the explanatory weight of the recovery model (Fig. 6B, and E to F). Mangroves recovered more quickly when they were further from human infrastructure.

The Western Caribbean subregion captured the best underlying effects of weather conditions in the year of cyclone damage and long-term climate trends on mangrove resilience. Thus, not only were mangroves in drier areas (381 mm) less likely to recover than those in wetter areas (460 mm), but those undergoing long-term drought also saw significant post-disturbance losses. Except for the Floridian subregion, all the other subregions experienced the same pattern of decreased resilience after tropical cyclone disturbances in areas with hotter and drier conditions (Fig. 6 and Tables A.12 to A.17).

Consistent with regional scale patterns, pre-cyclone forest structure affected resilience in all the subregions, with higher canopy densities, taller trees, and higher soil organic carbon stock promoting recovery. Exceptions included the Bahamian and the Western Caribbean subregions for tree height and the Southern Gulf of Mexico for canopy cover (where recovered and non-recovered mangroves had about 80 % of pre-disturbance green cover). Distance to the shoreline was an important variable to model recovery at the regional level, but there was no coherent response among the subregions (Fig. 6 and Tables A.12 to A.17).

Table 1
Original mangrove area in hectare (ha) (1), which was, *at least once*, impacted by tropical cyclones (2) and damaged (3) from 1996 to 2020, and recovered (4) and lost (5) from 1996 to 2019. Data are presented by subregion and summed for the entire North Atlantic Basin region.

Subregion	1. Original area (1996) (ha)	2. Impact (1996–2020)		3. Damage (1996–2020)			4. Recovery (1996–2019)			5. Loss (1996–2019)		
		(ha)	% Impact/ Original	(ha)	% Damage/ Original	% Damage/ Impact	(ha)	% Recovery/ Original	% Recovery/ Damage	(ha)	% Loss/ Original	% Loss/ Damage
Bahamian (BAH)	167,475	167,475	100	38,109	22.8	22.8	11,615	6.9	32.4	26,019	15.5	72.7
Eastern Caribbean (ECA)	87,945	87,945	100	2458	28.0	28.0	832	9.5	45.6	964	1.1	52.9
Floridian (FLO)	243,409	243,409	100	57,558	23.6	23.6	43,897	18.0	78.4	18,267	7.5	32.6
Greater Antilles (GAN)	489,790	489,790	100	104,037	21.2	21.2	54,498	11.1	53.5	45,920	9.4	45.1
Northern Gulf of Mexico (NGM)	12,098	12,098	100	662	5.5	5.5	81	0.7	60.4	53	0.4	39.8
Southern Caribbean (SCA)	52,552	12,428	23.6	85	n/a	n/a	33	n/a	n/a	46	n/a	n/a
Southern Gulf of Mexico (SGM)	559,204	556,451	99.5	38,425	6.9	6.9	16,304	2.9	50.5	18,990	3.4	58.9
Southwestern Caribbean (SWC)	175,322	67,160	38.3	8703	5.0	13.0	4973	2.8	63.1	3048	1.7	38.7
Western Caribbean (WCA)	316,650	316,645	100	29,877	9.4	9.4	9560	3.0	47.2	10,578	3.3	52.2
Total	2,025,295	1,874,257	92.5	279,914	13.8	14.9	141,793	7.0	55.4	123,885	6.1	48.4

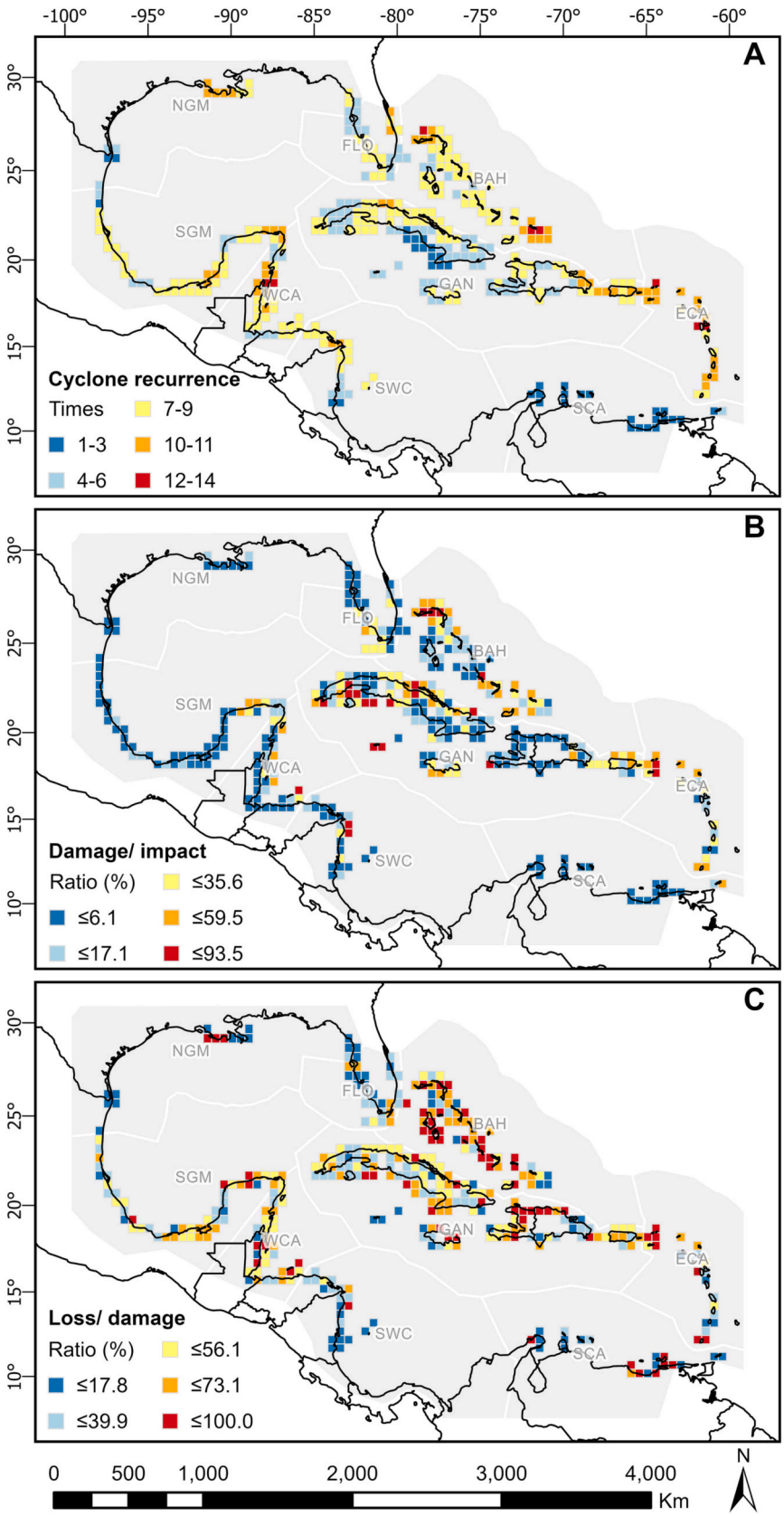

Fig. 3. Spatial distribution of cyclone recurrence (maximum recurrence) (A), damage ratios (damage/impact in percentage) (B), and post-disturbance loss ratios (loss/damage in percentage) (C) from 1996 to 2019 at each 0.5-degree cell. Subregion full names are listed in Table 1. Map lines delineate study areas and do not necessarily depict accepted national boundaries.

4. Discussion

4.1. Hotspots and drivers of mangrove response to tropical cyclones

We highlight that mangrove vulnerability and short-term resilience respond differently to cyclonic impacts in the North Atlantic Basin (NAB) region, consistent with known trade-offs between ecosystem resistance and resilience to tropical cyclones (Patrick et al., 2022). Mangroves showed low vulnerability (high resistance) to cyclones, with only ca. 15 % of the vastly impacted area being damaged, but rather low short-term resilience (48 % of loss) in areas damaged at least once. This is a large percentage for a region where mangroves have several post-disturbance adaptations, including rapid re-sprouting, prolific production of seedlings, fast rearrangements in species zonation, and rapid rates of succession and tree growth through their adaptive growth-mortality cycle (Jimenez et al., 1985). Thus, conservation, restoration, and adaptation efforts should focus on those more vulnerable mangroves and, most importantly, less resilient (as highlighted in Fig. 3).

There are marked subregional differences between mangrove damage and short-term loss, with east-west and north-south as the main axes. The highest ratios of damage ('damage/impact') are mostly concentrated in insular areas along the most preferential pathway of cyclones on the eastern side of the Caribbean: Eastern Caribbean (e.g., Guadeloupe, Grenada, Dominica), Bahamian, and Greater Antilles (e.g., Cuba, Puerto Rico) subregions. The southern part of the NAB experienced fewer impacts, less damage, and less loss. The western mangrove-rich subregions were also important when considering the absolute area of damaged mangroves. Therefore, the selected damage metrics play a key role in prioritizing action. On the other hand, less resilient mangroves with high 'loss/damage' ratios were more common in the Bahamian subregion, followed by sites in the Eastern Caribbean, Greater Antilles, Southern Gulf of Mexico, and Western Caribbean.

The characteristics of the cyclones (e.g., wind speed, rainfall) mainly drive vulnerability at the regional level. In contrast, short-term resilience is largely driven by site-specific conditions, including long-term climate conditions (e.g., drying trends and drier areas), pre-cyclone forest structure, soil, and human interventions on the land. The highest importance of wind speed to explain the vulnerability of mangroves

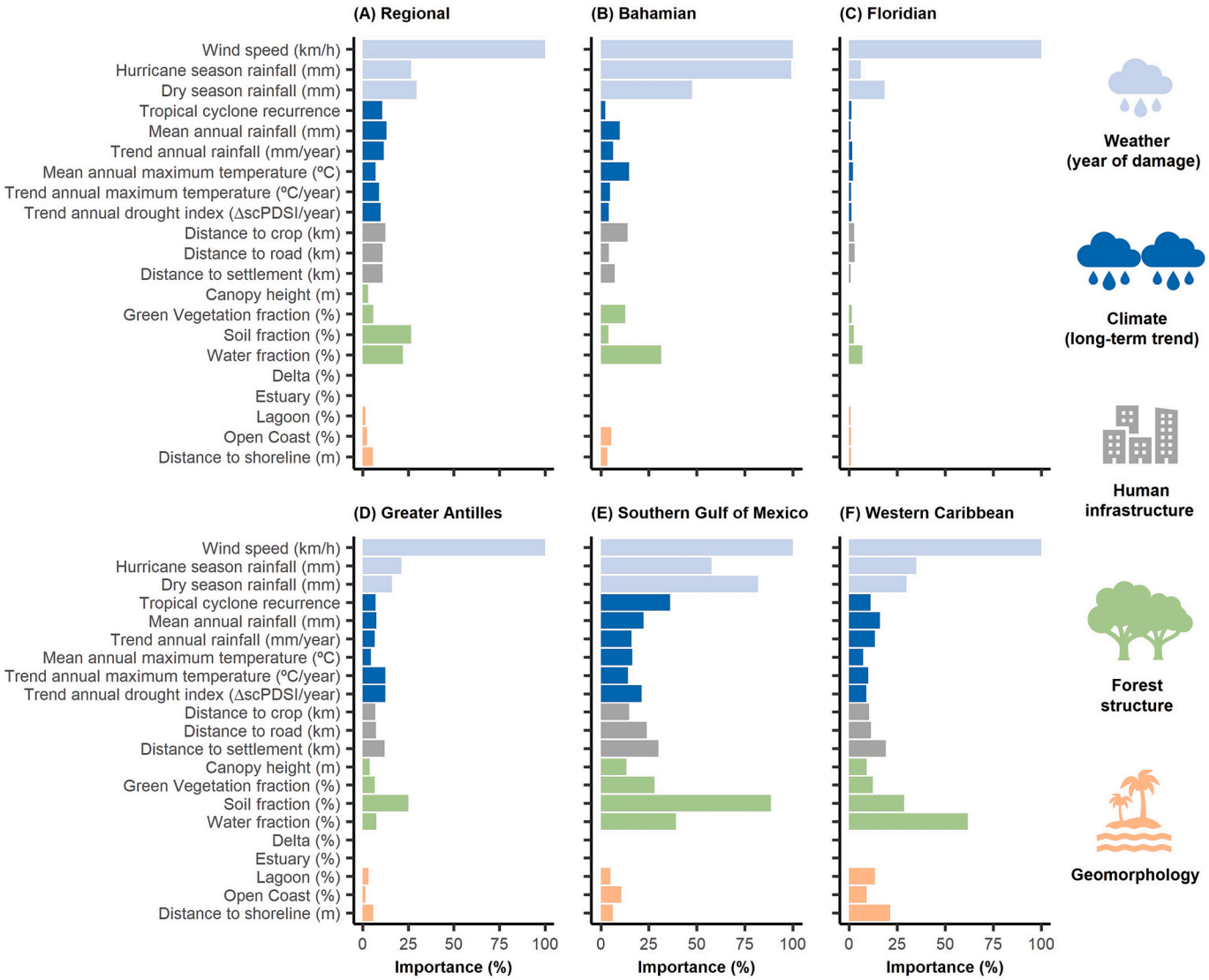

Fig. 4. Drivers of mangrove vulnerability at regional (A) and subregional scales (B—F) in the North Atlantic Basin (Gulf of Mexico and Caribbean). Bars are proportional to the variable importance from mangrove damaged vs. undamaged classification trees (n = 700). Five out of nine subregions (Spalding et al., 2007) are assessed here (i.e., those comprising ≥94 % of the mangrove extent in the NAB region: Bahamian, Floridian, Greater Antilles, Western Caribbean, and Southern Gulf of Mexico subregions). Data distributions are statistically different between classes (p-value ≤0.05) except for dry season rainfall and distance to settlement in the regional model and the trend of annual drought index in the Southern Gulf of Mexico and Western Caribbean models.

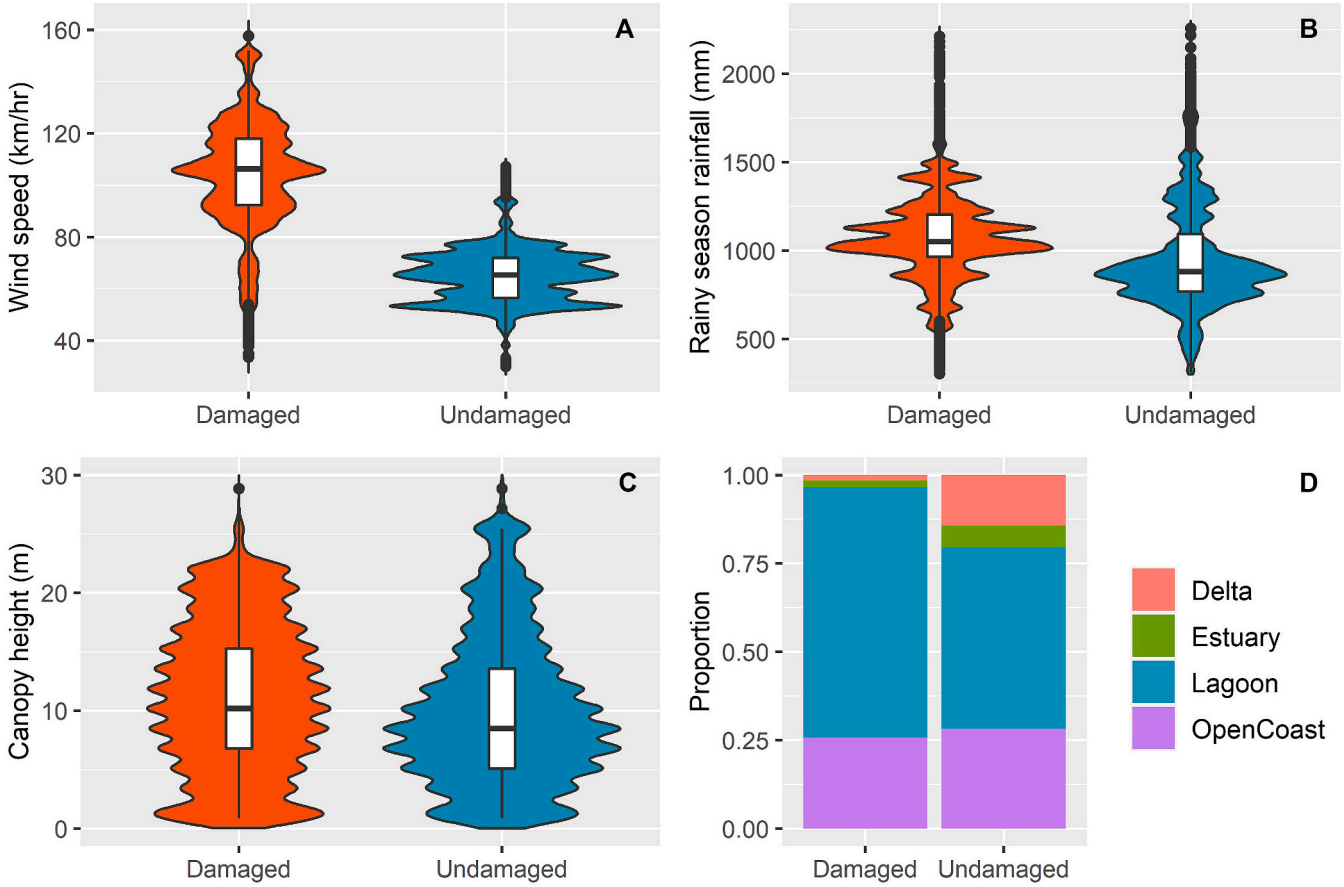

Fig. 5. Violin plots showing mangrove vulnerability (damaged vs. undamaged) in the NAB region (Caribbean and Gulf of Mexico) Maximum sustained wind speeds (A), cumulative rainfall in the hurricane (rainy) season (B), canopy height (C), and geomorphological unit (D). The lower and upper edges of the boxes indicate the interval between 25 and 75 % of the data distribution, and the central thick line is the median value. Horizontal lines outside the boxes indicate the minimum and maximum values of the dataset that were not outliers, and dots are outliers. Stacked bar plot showing the proportion (0–1) of regional "damaged" and "undamaged" samples per geomorphological setting (D).

was already presented in previous studies (e.g., Taillie et al., 2020). Winds can cause simple defoliation to uprooted trees, which alters the signal of greenness evaluated here. The Bahamian subregion was notable for its vulnerability to hurricane season rainfall. Its low-lying elevation (e.g., 80 % of the landmass is within 1.5 m of the mean sea level) and accelerated sea level rise (Kulp and Strauss, 2019; ECLA, 2020) seem to result in inundation conditions that affect mangrove survival. Depending on the intensity of the wind and rainfall, in association with the micro-environment mangrove is in (e.g., geomorphology), these weather variables may also affect the resilience of the ecosystem after damage making it unable to recover from the damage. Lagomasino et al. (2021) saw that mangrove dieback after the 2017 M-hurricane season was caused by ponding in South Florida. Geomorphology then influences mangroves' response to cyclone impact. The interaction between weather conditions and geomorphology seems to drive much of the vulnerability and resilience of mangroves through buried roots and increased salinity. This may be the case for lagoonal and basin mangroves, which present higher vulnerability and lower short-term resilience regionally. These mangroves might be experiencing unbalanced availability of fresh and salt water from increased sea level rise and reduced rainfall in the dry seasons.

Subregions with less human development close to mangroves, such as the Floridian, saw the greatest resilience. In contrast, the Bahamian subregion was characterized as least resilient, likely related to the compound effects of sea-level rise, topography, drought, and urbanization. The role of coastal development in mangrove vulnerability and loss of resilience can be associated with the chemical and physical changes that human infrastructure can have on the wetland ecosystem. Fertilizers from croplands and sewage from settlements may overfertilize the wetland ecosystem, while the construction of roads and settlements alters the tidal flushes and balance between fresh and saltwater (e.g., Harris et al., 2010; Feller et al., 2015). Mangrove vulnerability and resilience were most affected by human development and long-term climate (e.g., declining rainfall) in the Bahamian, Southern Gulf of Mexico, and Western Caribbean subregions. Both of these factors are expected to increase the exposure and vulnerability of ecosystems to extreme events (Sippo et al., 2018), and sites that face both stressors have been reported to exhibit magnified vulnerability in Mexico (Cinco-Castro and Herrera-Silveira, 2020).

The relationship between mangrove short-term loss and drought trends is relevant for managing and restoring cyclone-damaged mangroves in the NAB. In addition to including six of the driest countries in the world (FAO, 2016), large regions of Central America and the Caribbean are undergoing significant drying trends, and drying is projected to continue (Neelin et al., 2006). Our results are consistent with research on mangrove growth on a global scale, where the influence of precipitation was already highlighted as positively influencing mangrove growth (Simard et al., 2019a, 2019b). Thus, both long-term trends and extreme events of drought represent critical impacts on mangroves, mainly in arid subregions such as the Southern Gulf of Mexico, by increasing site salinity and decreasing mangrove ecophysiological capacity to adapt and be resilient (e.g., Zaldivar et al., 2000).

Several associations between mangrove response and environmental variables were found here with meaningful explanations. However, we

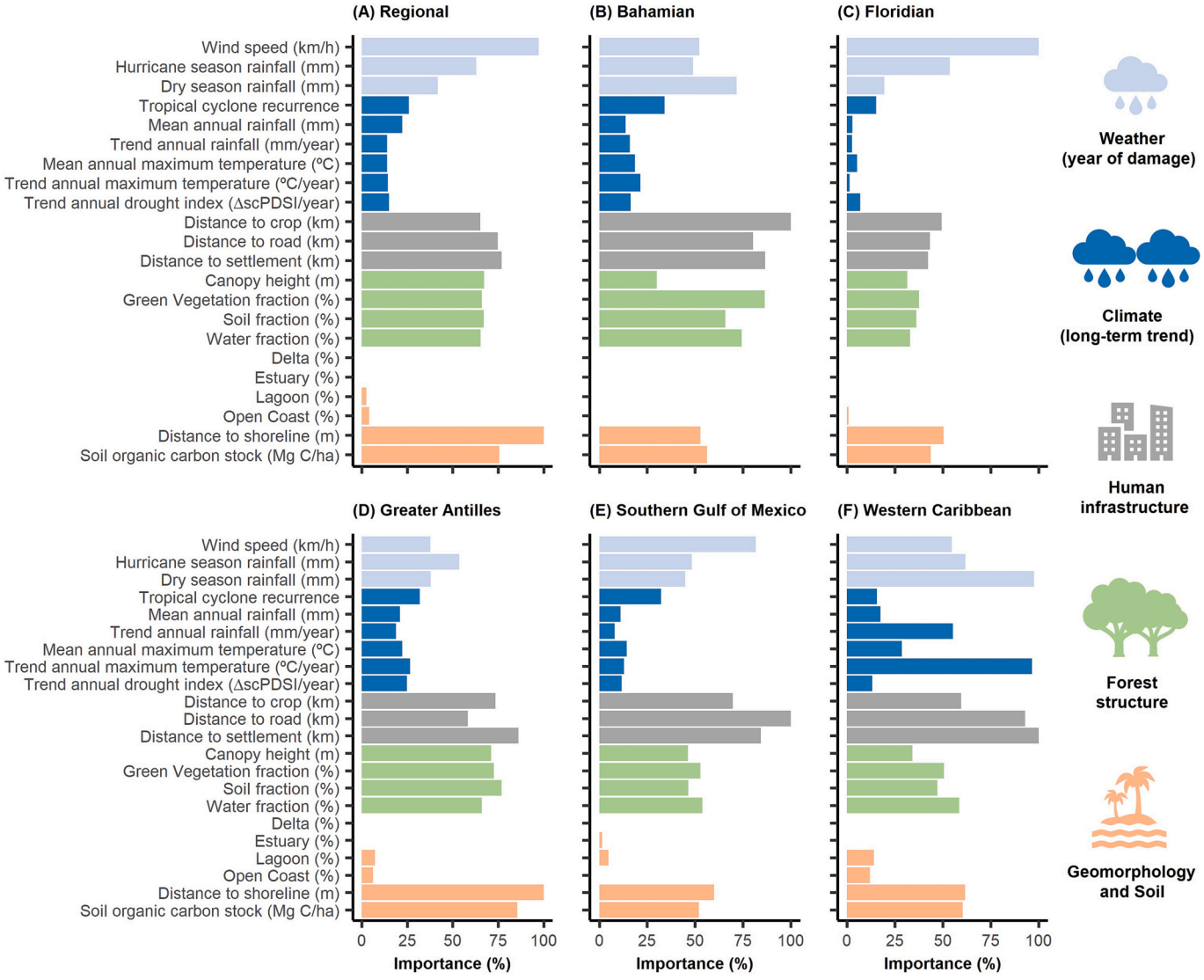

Fig. 6. Drivers of mangrove resilience at regional (A) and subregional scales (B-E) in the North Atlantic Basin (Gulf of Mexico and Caribbean). Bars are proportional to the variable importance from mangrove recovery vs. loss classification trees (n = 700). Five out of nine subregions (Spalding et al., 2007) are assessed here (i.e., those comprising ≥94 % of the mangrove extent in the NAB region: Bahamian, Floridian, Greater Antilles, Western Caribbean, and Southern Gulf of Mexico subregions). Data distributions are statistically different between classes (p-value ≤0.05) except for distance to road and to shoreline in the regional model, mean annual rainfall and maximum temperature, water fraction and distance to the shoreline in the Bahamian model, cyclone recurrence, soil fraction and distance to the shoreline in the Southern Gulf of Mexico model, and wind speed, cyclone recurrence, distance to settlement, canopy height, green and soil fractions and distance to the shoreline in the Western Caribbean model.

encourage further studies to explore the mechanisms behind these associations that may vary across regions and scales.

4.2. Limitations and uncertainties

Our results highlight the hotspots of mangrove vulnerability and loss of resilience from cyclone impact and the drivers of such responses throughout the NAB over 25 years of analysis. Analyses of this spatial-temporal extent and resolution have only recently become possible due to increased data availability and computing tools. To ensure effective environmental policy implementation, it is crucial to conduct long-term regional assessments. However, post hoc evaluation of results at a local scale is necessary for proper management.

Here we used 30-m-resolution NDVI to track variations in mangrove vegetation. It measures greenness and effectively captures the changes in ex-ante/ex-post canopy cover and the trends after disturbance. Our NDVI metrics are ground-validated and have already been published in several other papers (e.g., Lagomasino et al., 2019; Goldberg et al., 2020; Taillie et al., 2020; Adame et al., 2021; Lagomasino et al., 2021) as a mean to capturing mangrove greenness loss and gain. However, we acknowledge the limitations of using an index based on moderate-resolution surface reflectance to inform all kinds of mangrove damage and recovery. Thus, we recommend exploring other types of data, such as lidar measurements, to understand better the impacts of cyclones on forest structure (e.g., Xiong et al., 2022) even though they do not cover the entire region and period.

Uncertainties associated with global scale databases, such as the mangrove areas from the GMW product, should be expected. The product has an overall accuracy of 92.5 %, and factors such as satellite data availability, mangrove species composition, and level of degradation influence the mangrove map accuracy at a local scale (Bunting et al., 2018). The global mangrove forest height product used here also presents uncertainties, which are associated with discrepancies in the spatial scale, the timing of measurements, inherent GLAS and SRTM

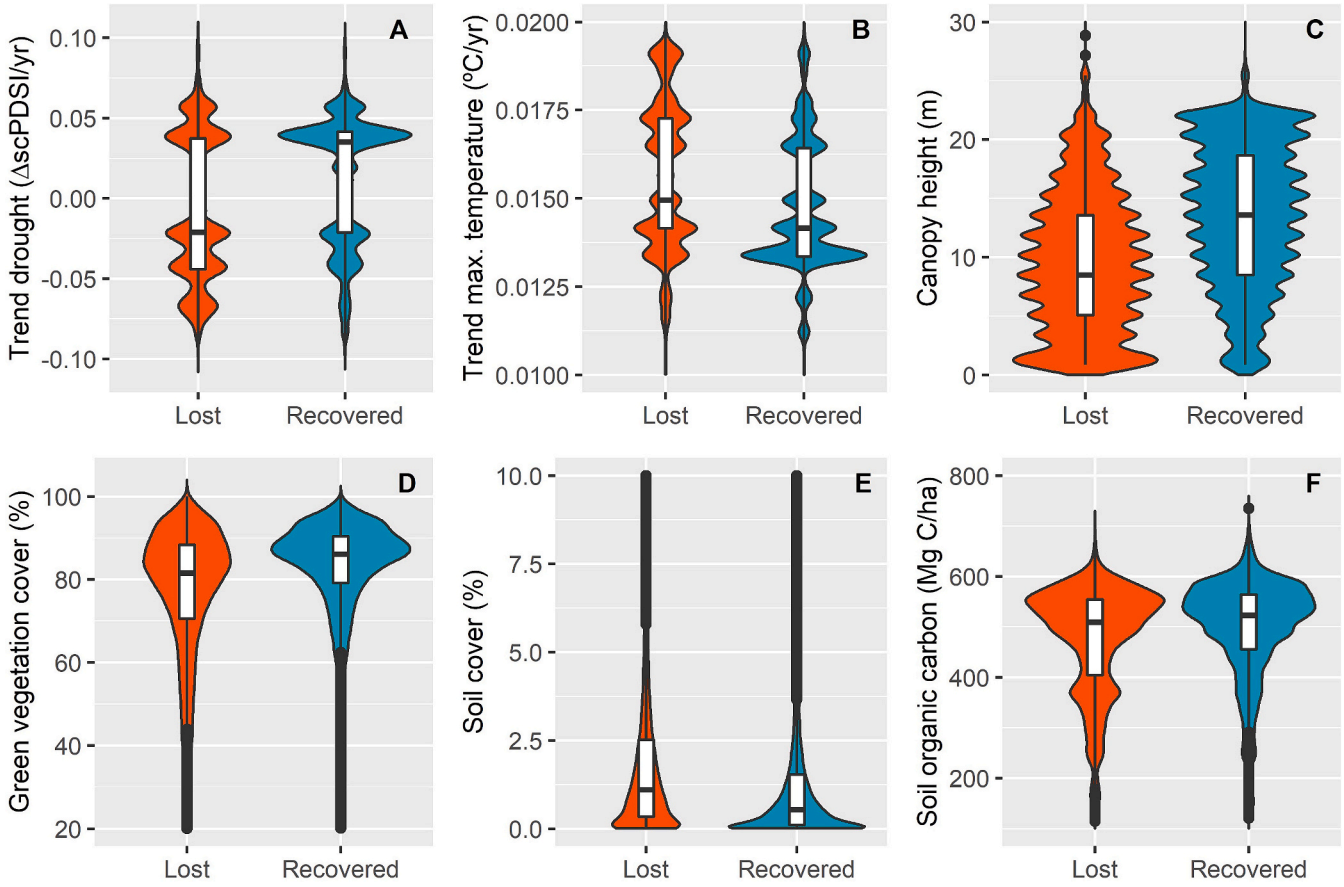

Fig. 7. Violin plots showing mangrove ex-post resilience responses (recovered vs. lost) in the NAB region. The long-term trend in Self-Calibrated Palmer Drought Severity Index (scPDSI) (A), the long-term trend in annual maximum temperature (B), canopy height (C), pre-cyclone green vegetation cover (D), pre-cyclone soil cover (D), and soil organic carbon stock (E). The lower and upper edges of the boxes indicate the interval between 25 and 75 % of the data distribution, and the central thick line is the median value. Horizontal lines outside the boxes indicate the minimum and maximum values of the dataset that were not outliers, and dots are outliers.

sensors' system errors, field measurement errors, geo-location errors, and discrepancies in spatial resolution between data (Simard et al., 2019a, 2019b). The RMSE of the lidar-based canopy height is 6.31 m.

Moderate to coarse resolution data type (>30-m resolution) also hinders us from capturing local-scale variations that can affect mangrove response to micro-environmental changes that a cyclone might produce. For example, geomorphological variation can influence mangrove dynamics across spatial scales. Furthermore, micro-geomorphological effects on mangrove response are associated with other elements such as aridity, karstic environment, and local changes caused by human intervention (Zaldivar et al., 2000; Osland et al., 2018; Harris et al., 2010).

Sea level rise can also interact with geomorphology to affect mangrove stability but was not considered in this study. We were limited by spatial data availability covering our study region over the 25 years of analysis. Similarly, both the human infrastructure data and vegetation height were considered static variables, despite clearly changing over time in reality. Nonetheless, we believe that those variables are less dynamic than others such as canopy cover, climate, and weather data that we addressed from bi-annual to seasonal time scales, respectively.

In addition, the vulnerability and resilience of mangroves on open coasts (27 % of the mangroves studied here) to tropical cyclones might also be affected by storm surges, waves' characteristics, and the consequent erosion. We suggest studies that concentrate on these geomorphic settings incorporate wave characteristics and simulate surges and erosion as variables for analysis.

4.3. Implications for management and regional policies

The resilience of both mangroves and socio-economic indicators in the NAB are predicted to decline. The observed increase in frequency and intensity of cyclones (Bacmeister et al., 2018; Emanuel, 2021; Wang and Toumi, 2021a, 2021b) we observed will likely become increasingly out of sync with recovery times: 1) the reported mangrove recovery times of 20 years (Lugo, 1980; Jimenez et al., 1985; Roth, 1992; Alongi, 2008; Krauss and Osland, 2020) and 2) the economic recovery time after extreme events in small economies such as the Antillean Islands (ca. 30 years) (Hsiang and Jina, 2014; López-Calva, 2019). Thus, environmental and socio-economic policies are needed to facilitate resilience in the NAB.

In addition, the compounding effects of simultaneous extreme events (ENSO droughts + hurricanes) and underlying climate trends (long-term drying + increasing cyclone frequency) are expected to enhance mortality. However, these compounding events require further study. Managers should therefore focus on enhancing mangrove adaptation to the compounding effects of climate change while also minimizing human drivers that can make mangroves more vulnerable and reduce their resilience after cyclone impacts (e.g., fragmentation, eutrophication, distance to roads, croplands, and settlements).

The impacts of increasing compound extreme events need to be framed in the context of heavy human influences in the region. Long-term losses of mangroves due to extreme events represented 20 % of the total mangrove deforestation in the NAB from 2000 to 2016 (Goldberg et al., 2020). While this contribution is significant and

extreme events play a role in ecosystem stability, the Caribbean has seen massive coastal tourism development in the last 70 years (Pattullo, 2005; Gmelch, 2012), which has long led to mangrove deforestation. These heavy human influences have increased the exposure and vulnerability of coastal communities to these extreme events (Cardona et al., 2012; Ramenzoni et al., 2020) and act as amplifiers of cyclone risks. Interestingly, distance to human infrastructure was less relevant in the Floridian mangroves. Even though this subregion has a high presence of settlements in the coastal zone, most of its mangroves are under protected status within the US Everglades National Park, which might be what makes them an exception in the region.

Living shorelines (mangroves, reefs, seagrasses, coastal marshes) provide more effective protection against cyclones and better facilitate post-disturbance socio-economic recovery than hard shorelines (Smith et al., 2018; Hochard et al., 2019; Menéndez et al., 2020; Zhu et al., 2020). While the region has multiple legal instruments to protect the coastal and marine ecosystems, donors have not yet fostered the value of Nature-based Solutions (NbS) (i.e., Green and Green-gray Infrastructures) in their regional budgets for post-disaster reconstruction, where mangrove conservation and restoration seem to remain unearmarked.

Our findings have direct implications for ecosystem conservation and coastal protection that interest a broad community of scientists and practitioners. The indication of the hotspots of mangrove losses due to cyclone damage and what are the drivers of such losses at a subregional scale might drive efforts to promote ecosystem functionality restoration following site-specific pressures and needs as part of risk reduction policies and as part of reconstruction funds after mega-hurricane seasons. The increased exposure of coastal communities to these natural hazards and inefficient policies for rapid response and recovery have led to devastating economic, social, physical, and mental health effects and, ultimately, massive migration in the region (e.g., Clark-Ginsberg et al., 2023). The effect of such hazards and environmental losses on economic-social vulnerability is exacerbated due to the region's complex local cultures, persistent and historical land grabbing, and the capitalism of disaster (Gutiérrez-Sánchez-Salamanca, 2023).

We particularly aim to raise awareness among coastal managers and donors to value the role of mangrove restoration and adaptive management – enhancing ecosystem resistance and resilience – as a fundamental regional NbS (Sowińska-Świerkosz and García, 2022) against climate change and extreme weather events, such as catastrophic cyclone hazards. Mangroves are essential to local communities due to their multiple ecosystem services, protecting them from flood, wind, and storm surges and providing them with food and work. Thus, maintaining mangroves healthy is basal to promoting resilience, equity, and sustainability in a well-known hazard-prone region with remarkable social and economic inequalities.

5. Conclusion

Mangroves are fundamental Nature-based Solutions against recurrent cyclone-related, socio-economic devastations in the North Atlantic Basin. In this study, we quantified the rates of cyclone impact, mangrove damage, and resilience loss across the North Atlantic Basin over twenty-five years of analysis. We also presented the drivers of such ecosystem responses at the regional and subregional levels. There are marked subregional differences in cyclone impact, mangrove damage, and short-term loss, with east-west and north-south as the main axes. Mangroves in the North Atlantic Basin experienced low vulnerability (high resistance) to cyclones but rather high short-term loss (low resilience) rates. While cyclone attributes drive regional vulnerability, site-specific conditions drive resilience. Areas undergoing long-term drought stand out for lower resilience from cyclone damage, and, at a subregional scale, coastal development influences both mangrove vulnerability and resilience to cyclones. Our results highlight the need to understand better the compounding effects of climate change and human infrastructure on this vital coastal ecosystem.

CRediT authorship contribution statement

Cibele Hummel do Amaral: Conceptualization, Methodology, Software, Formal analysis, Data curation, Writing – original draft, Visualization, Project administration. **Benjamin Poulter:** Conceptualization, Methodology, Writing – review & editing, Supervision, Project administration, Funding acquisition. **David Lagomasino:** Conceptualization, Methodology, Software, Resources, Writing – review & editing. **Temilola Fatoyinbo:** Conceptualization, Methodology, Software, Resources, Writing – review & editing. **Paul Taillie:** Conceptualization, Methodology, Software, Writing – review & editing. **Gil Lizcano:** Methodology, Software, Resources, Writing – review & editing. **Steven Canty:** Writing – review & editing, Funding acquisition. **Jorge Alfredo Herrera Silveira:** Writing – review & editing, Funding acquisition. **Claudia Teutli-Hernández:** Writing – review & editing. **Miguel Cifuentes:** Writing – review & editing, Funding acquisition. **Sean Patrick Charles:** Writing – review & editing. **Claudia Shantal Moreno:** Writing – review & editing. **Juan David González-Trujillo:** Writing – review & editing. **Rosa Maria Roman-Cuesta:** Conceptualization, Methodology, Resources, Writing – original draft, Supervision, Project administration, Funding acquisition.

Declaration of competing interest

The authors declare that they have no known competing financial interests or personal relationships that could have appeared to influence the work reported in this paper.

Data availability

Data will be made available on request.

Acknowledgments

This research was made possible thanks to the generous support from the BNP-PARIBAS Foundation on their 2019 Climate and Biodiversity Initiative call through the CORESCAM ("Coastal Biodiversity Resilience to Increasing Extreme Events in Central America") project. We thank Dr. Kamoru A. Lawal and Prof Mark New for providing long-term climate data and Prof. Helio Garcia Leite for assistance with the statistical analysis. We would like to thank the reviewers for their comments that enhanced the manuscript's quality.

Appendix A. Supplementary data

Supplementary data to this article can be found online at https://doi.org/10.1016/j.scitotenv.2023.165413.

References

Adame, M.F., Connolly, R.M., Turschwell, M.P., Lovelock, C.E., Fatoyinbo, T., Lagomasino, D., Brown, C.J., 2021. Future carbon emissions from global mangrove forest loss. Glob. Chang. Biol. 27 (12), 2856–2866.

Adams, J.B., Smith, M.O., Johnson, P.E., 1986. Spectral mixture modeling: a new analysis of rock and soil types at the Viking Lander 1 site. J. Geophys. Res. Solid Earth 91 (B8), 8098–8112.

Allen, K.J., Verdon-Kidd, D.C., Sippo, J.Z., Baker, P.J., 2021. Compound climate extremes driving recent sub-continental tree mortality in northern Australia have no precedent in recent centuries. Sci. Rep. 11 (1), 1–11.

Almeida, D.R.A., Broadbent, E.N., Ferreira, M.P., Meli, P., Zambrano, A.M.A., Gorgens, E. B., Brancalion, P.H., 2021. Monitoring restored tropical forest diversity and structure through UAV-borne hyperspectral and lidar fusion. Remote Sens. Environ. 264, 112582.

Alongi, D.M., 2008. Mangrove forests: resilience, protection from tsunamis, and responses to global climate change. Estuar. Coast. Shelf Sci. 76 (1), 1–13.

Bacmeister, J.T., Reed, K.A., Hannay, C., Lawrence, P., Bates, S., Truesdale, J.E., Levy, M., 2018. Projected changes in tropical cyclone activity under future warming scenarios using a high-resolution climate model. Clim. Chang. 146 (3), 547–560.

Berenguer, E., Lennox, G.D., Ferreira, J., Malhi, Y., Aragão, L.E., Barreto, J.R., Barlow, J., 2021. Tracking the impacts of El Niño drought and fire in human-modified Amazonian forests. Proc. Natl. Acad. Sci. 118 (30).
Brando, P.M., Balch, J.K., Nepstad, D.C., Morton, D.C., Putz, F.E., Coe, M.T., Soares-Filho, B.S., 2014. Abrupt increases in Amazonian tree mortality due to drought–fire interactions. Proc. Natl. Acad. Sci. 111 (17), 6347–6352.
Branoff, B.L., 2020. Mangrove disturbance and response following the 2017 hurricane season in Puerto Rico. Estuar. Coasts 43 (5), 1248–1262.
Breiman, L., 2001. Random forests. Mach. Learn. 45 (1), 5–32.
Bullock, E.L., Woodcock, C.E., Olofsson, P., 2020. Monitoring tropical forest degradation using spectral unmixing and Landsat time series analysis. Remote Sens. Environ. 238, 110968.
Bunting, P., Rosenqvist, A., Lucas, R.M., Rebelo, L.M., Hilarides, L., Thomas, N., Finlayson, C.M., 2018. The global mangrove watch—a new 2010 global baseline of mangrove extent. Remote Sens. 10 (10), 1669.
Cardona, O.D., Van Aalst, M.K., Birkmann, J., Fordham, M., Mc Gregor, G., Rosa, P., Thomalla, F., 2012. Determinants of risk: exposure and vulnerability. In: Managing the Risks of Extreme Events and Disasters to Advance Climate Change Adaptation: Special Report of the Intergovernmental Panel on Climate Change. Cambridge University Press, Cambridge, pp. 65–108.
Castañeda-Moya, E., Rivera-Monroy, V.H., Chambers, R.M., Zhao, X., Lamb-Wotton, L., Gorsky, A., Hiatt, M., 2020. Hurricanes fertilize mangrove forests in the Gulf of Mexico (Florida Everglades, USA). Proc. Natl. Acad. Sci. 117 (9), 4831–4841.
Center for International Earth Science Information Network (CIESIN), Columbia University, and Information Technology Outreach Services (ITOS)/University of Georgia, 2013. Global Roads Open Center (SEDAC). Retrieved from. http://sedac.ciesin.columbia.edu/data/set/groads-global-roadsopen-access-v1. September 15, 2020.
Center for International Earth Science Information Network - CIESIN - Columbia University, Information Technology Outreach Services - ITOS - University of Georgia, 2013. Global Roads Open Access Data Set, Version 1 (gROADSv1). Palisades, New York: NASA Socioeconomic Data and Applications Center (SEDAC). https://doi.org/10.7927/H4VD6WCT. Accessed on 08/20/2020.
Center For International Earth Science Information Network (CIESIN), Columbia University, International Food Policy Research Institute (IFPRI), The World Bank, Centro Internacional De Agricultura Tropical (CIAT), 2011. Global Rural-Urban Mapping Project, Version 1 (GRUMPv1): Settlement Points. Retrieved from. https://sedac.ciesin.columbia.edu/data/collection/grump-v1. September 15, 2020.
Center For International Earth Science Information Network - CIESIN - Columbia University, International Food Policy Research Institute (IFPRI), The World Bank, Centro Internacional De Agricultura Tropical (CIAT), 2011. Global Rural-Urban Mapping Project, Version 1 (GRUMPv1): Settlement Points. Palisades, New York: NASA Socioeconomic Data and Applications Center (SEDAC). https://doi.org/10.7927/H4M906KR. Accessed on 08/20/2020.
Cinco-Castro, S., Herrera-Silveira, J., 2020. Vulnerability of mangrove ecosystems to climate change effects: the case of the Yucatan peninsula. Ocean Coast. Manag. 192, 105196.
Clark-Ginsberg, A., Sprague Martinez, L., Scaramutti, C., Rodríguez, J., Salas-Wright, C. P., Schwartz, S.J., 2023. Social vulnerability shapes the experiences of climate migrants displaced by Hurricane Maria. Clim. Dev. 1–11.
Danielson, T.M., Rivera-Monroy, V.H., Castañeda-Moya, E., Briceño, H., Travieso, R., Marx, B.D., Farfán, L.M., 2017. Assessment of Everglades mangrove forest resilience: implications for above-ground net primary productivity and carbon dynamics. For. Ecol. Manag. 404, 115–125.
Dennison, P.E., Roberts, D.A., 2003. Endmember selection for multiple endmember spectral mixture analysis using endmember average RMSE. Remote Sens. Environ. 87 (2–3), 123–135.
Donato, D.C., Kauffman, J.B., Murdiyarso, D., Kurnianto, S., Stidham, M., Kanninen, M., 2011. Mangroves among the most carbon-rich forests in the tropics. Nat. Geosci. 4 (5), 293–297.
Earth Security, 2020. Financing the earth's assets: the case for mangroves as a nature-based climate solution, 66pp. https://earthsecurity.org/wp-content/uploads/2020/12/2128_ESG_mangrove_22.pdf.
Economic Commission for Latin America and the Caribbean, 2018. Irma and Maria by Numbers. FOCUS ECLA in the Caribbean, Port of Spain, 16pp. https://repositorio.cepal.org/bitstream/handle/11362/43446/1/FOCUSIssue1Jan-Mar2018.pdf, 16pp.
Economic Commission for Latin America and the Caribbean, 2020. Assessment of the Effects and Impacts of Hurricane Dorian in the Bahamas. FOCUS ECLA in the Caribbean, Port of Spain, 219pp. https://repositorio.cepal.org/bitstream/handle/11362/45968/4/S2000587_en.pdf.
Emanuel, K., 2021. Atlantic tropical cyclones downscaled from climate reanalyses show increasing activity over past 150 years. Nat. Commun. 12 (1), 1–8.
Feller, I.C., Dangremond, E.M., Devlin, D.J., Lovelock, C.E., Proffitt, C.E., Rodriguez, W., 2015. Nutrient enrichment intensifies hurricane impact in scrub mangrove ecosystems in the Indian River Lagoon, Florida, USA. Ecology 96 (11), 2960–2972.
FOOD AND AGRICULTURE ORGANIZATION OF THE UNITED NATIONS - FAO, 2016. Drought Characteristics and Management in the Caribbean. FAO WATER REPORTS, Rome, p. 42, 77pp. https://www.fao.org/3/i5695e/i5695e.pdf, 77pp.
Gijsman, R., Horstman, E.M., van der Wal, D., Friess, D.A., Swales, A., Wijnberg, K.M., 2021. Nature-based engineering: a review on reducing coastal flood risk with mangroves. Front. Mar. Sci. 8.
Gmelch, G., 2012. Behind the Smile: The Working Lives of Caribbean Tourism, 2nd ed. Indiana University Press, Bloomington. 256 pp.
Goldberg, L., Lagomasino, D., Thomas, N., Fatoyinbo, T., 2020. Global declines in human-driven mangrove loss. Glob. Chang. Biol. 26 (10), 5844–5855.
Gorelick, N., Hancher, M., Dixon, M., Ilyushchenko, S., Thau, D., Moore, R., 2017. Google Earth Engine: planetary-scale geospatial analysis for everyone. Remote Sens. Environ. 202, 18–27.
Gutiérrez-Sánchez-Salamanca, E., 2023. Analysing climate migration dynamics in the Caribbean through the iota hurricane: Shock doctrine, capitalism of disasters and development. In: Global Climate Change and Environmental Refugees. Springer, Cham, pp. 137–184.
Hall, T.M., Kossin, J.P., 2019. Hurricane stalling along the North American coast and implications for rainfall. Clim. Atmos. Sci. 2 (1), 1–9.
Harris, R.J., Milbrandt, E.C., Everham, E.M., Bovard, B.D., 2010. The effects of reduced tidal flushing on mangrove structure and function across a disturbance gradient. Estuar. Coasts 33 (5), 1176–1185.
Hayashi, S.N., Souza-Filho, P.W.M., Nascimento Jr., W.R., Fernandes, M.E., 2019. The effect of anthropogenic drivers on spatial patterns of mangrove land use on the Amazon coast. PLoS One 14 (6), e0217754.
Hersbach, H., Bell, B., Berrisford, P., Biavati, G., Horányi, A., Muñoz Sabater, J., Nicolas, J., Peubey, C., Radu, R., Rozum, I., Schepers, D., Simmons, A., Soci, C., Dee, D., Thépaut, J.-N., 2018. ERA5 hourly data on single levels from 1959 to present. In: Copernicus Climate Change Service (C3S) Climate Data Store (CDS).
Hersbach, H., Bell, B., Berrisford, P., Biavati, G., Horányi, A., Muñoz Sabater, J., Nicolas, J., Peubey, C., Radu, R., Rozum, I., Schepers, D., Simmons, A., Soci, C., Dee, D., Thépaut, J-N., 2023. ERA5 hourly data on single levels from 1940 to present. Copernicus Climate Change Service (C3S) Climate Data Store (CDS). http://10.24381/cds.adbb2d47. Accessed on 08/20/2020.
Hochard, J.P., Hamilton, S., Barbier, E.B., 2019. Mangroves shelter coastal economic activity from cyclones. Proc. Natl. Acad. Sci. 116 (25), 12232–12237.
Hsiang, S.M., Jina, A.S., 2014. The Causal Effect of Environmental Catastrophe on Long-Run Economic Growth: Evidence from 6,700 Cyclones (No. w20352). National Bureau of Economic Research. https://www.nber.org/system/files/working_papers/w20352/w20352.pdf.
Imbert, D., 2018. Hurricane disturbance and forest dynamics in East Caribbean mangroves. Ecosphere 9 (7), e02231.
Ingrisch, J., Bahn, M., 2018. Towards a comparable quantification of resilience. Trends Ecol. Evol. 33 (4), 251–259.
Jimenez, J.A., Lugo, A.E., Cintron, G., 1985. Tree mortality in mangrove forests. Biotropica 17 (3), 177–185.
Knapp, K.R., Kruk, M.C., Levinson, D.H., Diamond, H.J., Neumann, C.J., 2010. The international best track archive for climate stewardship (IBTrACS): unifying tropical cyclone best track data. Bull. Am. Meteorol. Soc. 91, 363–376.
Knutson, T.R., Chung, M.V., Vecchi, G., Sun, J., Hsieh, T.L., Smith, A., 2021. Climate change is probably increasing the intensity of tropical cyclones. In: Critical Issues in Climate Change Science. ScienceBrief Review. https://tyndall.ac.uk/wp-content/uploads/2021/03/sciencebrief_review_cyclones_mar2021.pdf.
Krauss, K.W., Osland, M.J., 2020. Tropical cyclones and the organization of mangrove forests: a review. Ann. Bot. 125 (2), 213–234.
Kuhn, M., 2012. Variable importance using the caret package. J. Stat. Softw. 6.
Kuhn, M., Wing, J., Weston, S., Williams, A., Keefer, C., Engelhardt, A., Benesty, M., 2020. Package 'caret'. The R J. 223.
Kulp, S.A., Strauss, B.H., 2019. New elevation data triple estimates of global vulnerability to sea-level rise and coastal flooding. Nat. Commun. 10 (1), 1–12.
Lagomasino, D., Fatoyinbo, T., Lee, S., Feliciano, E., Trettin, C., Shapiro, A., Mangora, M. M., 2019. Measuring mangrove carbon loss and gain in deltas. Environ. Res. Lett. 14 (2), 025002.
Lagomasino, D., Fatoyinbo, T., Castañeda-Moya, E., Cook, B.D., Montesano, P.M., Neigh, C.S., Morton, D.C., 2021. Storm surge and ponding explain mangrove dieback in southwest Florida following Hurricane Irma. Nat. Commun. 12 (1), 1–8.
Landsea, C. W, & Franklin, J. L. n.d. "Atlantic hurricane database uncertainty and presentation of a new database format." Accessed July 19, 2019. doi:https://doi.org/10.1175/MWR-D-12-00254.1.
López-Calva, L. F. (2019, March 21). After the Rain: The Lasting Effects of Storms in the Caribbean. UNDP Latin America and the Caribbean. https://www.latinamerica.undp.org/content/rblac/en/home/presscenter/director-s-graph-for-thought/los-danos-por-tormenta-en-el-caribe.html.
Lugo, A.E., 1980. Mangrove ecosystems: successional or steady state? Biotropica 12 (2), 65–72.
Massey, R., Sankey, T.T., Yadav, K., Congalton, R.G., Tilton, J.C., Thenkabail, P.S., 2017. NASA Making Earth System Data Records for Use in Research Environments (MEaSUREs). Global Food Security-support Analysis Data (GFSAD). Cropland Extent 2010 North America 30 m V001. NASA EOSDIS Land Processes DAAC. https://doi.org/10.5067/MEaSUREs/GFSAD/GFSAD30NACE.001.
Mazda, Y., Magi, M., Kogo, M., Hong, P.N., 1997. Mangroves as a coastal protection from waves in the Tong King delta, Vietnam. In: Mangroves and Salt Marshes, 1, pp. 127–135.
McIvor, A.L., Möller, I., Spencer, T., Spalding, M., 2012. Reduction of wind and swell waves by mangroves. In: Natural Coastal Protection Series: Report 1. Cambridge Coastal Research Unit Working Paper 40 (ISSN 2050-7941).
Méndez-Alonzo, R., Moctezuma, C., Ordoñez, V.R., Angeles, G., Martínez, A.J., López-Portillo, J., 2015. Root biomechanics in Rhizophora mangle: anatomy, morphology and ecology of mangrove's flying buttresses. Ann. Bot. 115 (5), 833–840.
Menéndez, P., Losada, I.J., Torres-Ortega, S., Narayan, S., Beck, M.W., 2020. The global flood protection benefits of mangroves. Sci. Rep. 10 (1), 1–11.
Montgomery, J.M., Bryan, K.R., Mullarney, J.C., Horstman, E.M., 2019. Attenuation of storm surges by coastal mangroves. Geophys. Res. Lett. 46 (5), 2680–2689.
Neelin, J.D., Münnich, M., Su, H., Meyerson, J.E., Holloway, C.E., 2006. Tropical drying trends in global warming models and observations. Proc. Natl. Acad. Sci. 103 (16), 6110–6115.

Osland, M.J., Feher, L.C., López-Portillo, J., Day, R.H., Suman, D.O., Menéndez, J.M.G., Rivera-Monroy, V.H., 2018. Mangrove forests in a rapidly changing world: global change impacts and conservation opportunities along the Gulf of Mexico coast. Estuar. Coast. Shelf Sci. 214, 120–140.
Ötker, İ., Srinivasan, K., 2018. Bracing for the storm: for the Caribbean, building resilience is a matter of survival. Finance Dev. 55 (001).
Patrick, C.J., Kominoski, J.S., McDowell, W.H., Branoff, B., Lagomasino, D., Leon, M., Zou, X., 2022. A general pattern of trade-offs between ecosystem resistance and resilience to tropical cyclones. Sci. Adv. 8 (9), eabl9155.
Pattullo, P., 2005. Last Resorts: The Cost of Tourism in the Caribbean, 2nd ed. NYU Press, New York, p. 274.
Peereman, J., Hogan, J.A., Lin, T.C., 2022. Disturbance frequency, intensity and forest structure modulate cyclone-induced changes in mangrove forest canopy cover. Glob. Ecol. Biogeogr. 31 (1), 37–50.
R Core Team, 2020. R: A Language and Environment for Statistical Computing. R Foundation for Statistical Computing, Vienna, Austria. https://www.R-project.org/.
Ramenzoni, V.C., Borroto Escuela, D., Rangel Rivero, A., González-Díaz, P., Vázquez Sánchez, V., López-Castañeda, L., Yoskowitz, D., 2020. Vulnerability of fishery-based livelihoods to extreme events: local perceptions of damages from hurricane Irma and tropical storm Alberto in Yaguajay, Central Cuba. Coast Manage. 48 (5), 354–377.
Richards, D.R., Thompson, B.S., Wijedasa, L., 2020. Quantifying net loss of global mangrove carbon stocks from 20 years of land cover change. Nat. Commun. 11 (1), 1–7.
Rivera-Monroy, V.H., Farfán, L.M., Brito-Castillo, L., Cortés-Ramos, J., González-Rodríguez, E., D'Sa, E.J., Euan-Avila, J.I., 2020. Tropical cyclone landfall frequency and large-scale environmental impacts along karstic coastal regions (Yucatan Peninsula, Mexico). Appl. Sci. 10 (17), 5815.
Roth, L.C., 1992. Hurricanes and mangrove regeneration: effects of hurricane Joan, October 1988, on the vegetation of Isla del Venado, Bluefields, Nicaragua. Biotropica 375–384.
Sanderman, J., Hengl, T., Fiske, G., Solvik, K., Adame, M.F., Benson, L., Landis, E., 2018. A global map of mangrove forest soil carbon at 30 m spatial resolution. Environ. Res. Lett. 13 (5), 055002.
Simard, M., Fatoyinbo, T., Smetanka, C., Rivera-monroy, V.H., Castaneda, E., Thomas, N., Van der stocken, T., 2019a. Global Mangrove Distribution, Aboveground Biomass, and Canopy Height. ORNL DAAC, Oak Ridge, Tennessee, USA. https://doi.org/10.3334/ORNLDAAC/1665.
Simard, M., Fatoyinbo, L., Smetanka, C., Rivera-Monroy, V.H., Castañeda-Moya, E., Thomas, N., Van der Stocken, T., 2019b. Mangrove canopy height globally related to precipitation, temperature and cyclone frequency. Nat. Geosci. 12 (1), 40–45.
Sippo, J.Z., Lovelock, C.E., Santos, I.R., Sanders, C.J., Maher, D.T., 2018. Mangrove mortality in a changing climate: an overview. Estuar. Coast. Shelf Sci. 215, 241–249.
Smith, T.J., Anderson, G.H., Balentine, K., Tiling, G., Ward, G.A., Whelan, K.R., 2009. Cumulative impacts of hurricanes on Florida mangrove ecosystems: sediment deposition, storm surges and vegetation. Wetlands 29 (1), 24–34.
Smith, C.S., Puckett, B., Gittman, R.K., Peterson, C.H., 2018. Living shorelines enhanced the resilience of saltmarshes to Hurricane Matthew (2016). Ecol. Appl. 28 (4), 871–877.
Sowińska-Świerkosz, B., & García, J. (2022). What are nature-based solutions (NBS)? Setting core ideas for concept clarification. Nature-Based Solutions, 2, 100009.
Spalding, M.D., Fox, H.E., Allen, G.R., Davidson, N., Ferdaña, Z.A., Finlayson, M.A.X., Robertson, J., 2007. Marine ecoregions of the world: a bioregionalization of coastal and shelf areas. BioScience 57 (7), 573–583.
Spatz, H.C., Brinkman, A.G., Smit, J.H., 1987. Biomechanical adaptations of two Caribbean mangrove trees to the physical stress of sedimentation. Am. J. Bot. 74 (2), 183–191.
Taillie, P.J., Roman-Cuesta, R., Lagomasino, D., Cifuentes-Jara, M., Fatoyinbo, T., Ott, L. E., Poulter, B., 2020. Widespread mangrove damage resulting from the 2017 Atlantic mega hurricane season. Environ. Res. Lett. 15 (6), 064010.
Thampanya, U., Vermaat, J.E., Sinsakul, S., Panapitukkul, N., 2006. Coastal erosion and mangrove progradation of southern Thailand. Estuar. Coast. Shelf Sci. 68 (1–2), 75–85.
Tomiczek, T., Wargula, A., Hurst, N.R., Bryant, D.B., Provost, L.A., 2021. Engineering With Nature: the role of mangroves in coastal protection, 19pp. https://ewn.erdc.dren.mil/wp-content/uploads/2021/11/ERDC-TN_EWN-21-1_Mangroves.pdf.
Tomlinson, P.B., 2016. The Botany of Mangroves. Cambridge University Press, 432pp.
University of East Anglia Climatic Research Unit (CRU), Harris, I.C., Jones, P.D., 2017. *CRU TS3.25*: Climatic Research Unit (CRU) Time-Series (TS) Version 3.25 of High-Resolution Gridded Data of Month-by-month Variation in Climate (Jan. 1901- Dec. 2016). Centre for Environmental Data Analysis, 05 December 2017.
Van Hespen, R., Hu, Z., Borsje, B., De Dominicis, M., Friess, D.A., Jevrejeva, S., Bouma, T. J., 2023. Mangrove forests as a nature-based solution for coastal flood protection: biophysical and ecological considerations. Water Sci. Eng. 16 (1), 1–13.
Villate Daza, D.A., Sánchez Moreno, H., Portz, L., Portantiolo Manzolli, R., Bolívar-Anillo, H.J., Anfuso, G., 2020. Mangrove forests evolution and threats in the Caribbean sea of Colombia. Water 12 (4), 1113.
Vogt, J., Skóra, A., Feller, I.C., Piou, C., Coldren, G., Berger, U., 2012. Investigating the role of impoundment and forest structure on the resistance and resilience of mangrove forests to hurricanes. Aquat. Bot. 97 (1), 24–29.
Wang, S., Toumi, R., 2021a. Recent migration of tropical cyclones toward coasts. Science 371 (6528), 514–517.
Wang, S., Toumi, R., 2021b. Recent tropical cyclone changes inferred from ocean surface temperature cold wakes. Sci. Rep. 11 (1), 1–8.
Worthington, T.A., Zu Ermgassen, P.S., Friess, D.A., Krauss, K.W., Lovelock, C.E., Thorley, J., Spalding, M., 2020. A global biophysical typology of mangroves and its relevance for ecosystem structure and deforestation. Sci. Rep. 10 (1), 1–11.
Xiong, L., Lagomasino, D., Charles, S.P., Castañeda-Moya, E., Cook, B.D., Redwine, J., Fatoyinbo, L., 2022. Quantifying mangrove canopy regrowth and recovery after Hurricane Irma with large-scale repeat airborne lidar in the Florida Everglades. Int. J. Appl. Earth Obs. Geoinf. 114, 103031.
Yengoh, G.T., Dent, D., Olsson, L., Tengberg, A.E., Tucker III, C.J., 2015. Use of the Normalized Difference Vegetation Index (NDVI) to Assess Land Degradation at Multiple Scales: Current Status, Future Trends, and Practical Considerations. Springer. https://doi.org/10.1007/978-3-319-24112-8, 80p.
Zaldivar, A., Herrera-Silveira, J.A., Capurro, L., 2000. Soil salinity and community structure of two mangrove forests in Yucatan, Southeastern Mexico. Internationale Vereinigung für theoretische und angewandte Limnologie: Verhandlungen 27 (3), 1707–1710.
Zhai, A.R., Jiang, H.J., 2014. Dependence of US Hurricane Economic Loss on Maximum Wind Speed and Storm Size. https://doi.org/10.1088/1748-9326/9/6/064019.
Zhong, Y., Giri, C., Thenkabail, P.S., Teluguntla, P., Congalton, R.G., Yadav, K., Oliphant, A.J., Xiong, J., Poehnelt, J., Smith, C., 2017. NASA Making Earth System Data Records for Use in Research Environments (MEaSUREs). Global Food Security-support Analysis Data (GFSAD). Cropland Extent 2015 South America 30 m V001. NASA EOSDIS Land Processes DAAC. https://doi.org/10.5067/MEaSUREs/GFSAD/GFSAD30SACE.001.
Zhu, Z., Vuik, V., Visser, P.J., Soens, T., van Wesenbeeck, B., van de Koppel, J., Bouma, T. J., 2020. Historic storms and the hidden value of coastal wetlands for nature-based flood defence. Nat. Sustain. 3 (10), 853–862.